Advanced Composites and Hybrid Materials (2023) 6:130
https://doi.org/10.1007/s42114-023-00678-5

REVIEW

Overview of emerging hybrid and composite materials for space applications

J. C. Ince[1] · M. Peerzada[2] · L. D. Mathews[1] · A. R. Pai[3] · A. Al-qatatsheh[1] · S. Abbasi[1] · Y. Yin[1] · N. Hameed[1] · A. R. Duffy[4] · A. K. Lau[5] · N. V. Salim[1]

Received: 31 July 2022 / Revised: 13 April 2023 / Accepted: 23 April 2023 / Published online: 26 June 2023

Abstract
Space exploration is one of humanity's most challenging and costly activities. Nevertheless, we continuously strive to venture further and more frequently into space. It is vital to make every effort to minimise and mitigate the risks to astronaut safety, expand the long-term operation of technologies in space and improve the overall feasibility of space exploration—this calls for an assessment of recent advances in materials with applications in space. This review focuses on state-of-the-art materials that address challenges, threats and risks experienced during space exploration. Said challenges considered in this review include the danger of micro-meteorites, fire in space, space dust, temperature extremes, electromagnetic interference (EMI) and the cost associated with space travel. The materials discussed include self-healing polymers, fire and thermally resistant materials, materials for thermal management, self-cleaning materials, EMI shielding materials and multifunctional carbon fibre composites. Through this catalogue, we seek to inform and suggest the future direction of advancing space exploration by selecting innovative materials.

Keywords Emerging materials · Self-repair · EMI shielding · Dust mitigation · Thermal management · Smart composites

1 Introduction

Space is perhaps the most unforgiving, uninhabitable, hazardous and costly environment to explore. Without the tremendous engineering efforts of the space race, which commenced in the 1950s, space exploration would not be possible due to the unique challenges experienced during space travel. Yet despite said efforts, space still poses many risks to astronaut safety and mission success. Whilst much work was conducted to develop novel functional materials for mitigating the challenges of space—the advent of Teflon being a well-known example—largely, materials that were already commercially available were repurposed or modified for a given application. Nowadays, materials are being designed and engineered specifically to solve challenges experienced in spacecraft engineering and exploration. Concurrently, materials science (nanomaterials science in particular) is a booming field of research. Researchers are now developing advanced materials with superb functionalities and, in many instances, even multifunctionality. This is increasingly facilitating the potential for safer, more economical, feasible and durable spacecraft and space exploration missions—the Overton window is poised for the fruition of the next generation of spacecraft. The question then remains to be, what risks can be addressed with the so-called emerging advanced materials for spacecraft engineering and exploration, what are these materials and how can these materials be utilised in spacecraft engineering to mitigate the risks and hazards of space exploration?

One of the largest risks in space is the possibility of high-velocity impacts from space debris or micro-meteoroids. These objects can travel at velocities of 42 km s^{-1} and can tear apart spacecraft upon impact, causing air leaks and

JC Ince and M Peerzhada contributed equally to this work.

✉ N. V. Salim
nsalim@swin.edu.au

[1] School of Engineering, Swinburne University of Technology, Hawthorn, Australia

[2] Institute of Advanced Engineering and Space Sciences, University of Southern Queensland, Toowoomba 4350, Australia

[3] International and Inter University Centre for Nanoscience and Nanotechnology, Mahatma Gandhi University, Kottayam, Kerala 686560, India

[4] Centre for Astrophysics and Supercomputing, Swinburne University of Technology, Melbourne, VIC 3122, Australia

[5] Technological and Higher, Education Institute of Hong Kong, Chai Wan, Hong Kong SAR, China

threatening astronaut safety, spacecraft longevity and mission success. Near-Earth orbit is riddled with these objects; approximately 27,000 10-cm or larger objects have been detected. The Union of Concerned Scientists states that 3372 active satellites orbit Earth [1]. As this number will soon significantly rise, scientists must seek novel solutions to mitigate the threat of high-velocity impacts. The recent Canadarm2 incident, where an unknown object smashed into a robotic arm, highlights the growing threat of orbital debris, spent rocket parts and other wayward objects. Spacecraft are therefore logically engineered from mechanically robust materials to protect the spacecraft from high-velocity impacts. But since the shear impact velocity of small objects in near-Earth orbit can be 10,000 times faster than the muzzle velocity of bullets, engineering materials that can withstand such impacts is an incredible challenge. Ergo, rather than engineering materials that can withstand such impacts, scientists are instead developing materials that can repair automatically in the event of an impact, so-called self-healing materials [2, 3]. In addition to the threat of high-velocity impacts, self-healing materials are also being explored to address damages incurred to spacecraft components due to atomic oxygen, vacuum ultraviolet radiation and extreme temperatures so that spacecraft are safer, have improved longevity and are more economical.

Fire is extremely hazardous in the best of conditions, but in space, the threat of fire is amplified. If a fire occurs in space, the cabin is rich in oxygen which quickens the propagation of the fire. Once a fire is out of control, there is virtually no escape. In conjunction, spacecraft are abundant with sensitive electronics, circuits and wiring harnesses which are critical to the operation of the spacecraft and the onboard astronaut life support system. If a fire occurs, these systems can be damaged, posing a threat to astronauts even if the fire is extinguished. The causes of fires in space generally stem from atmospheric friction, electrical and heating overload and ignition of waste. All these causes are difficult to eliminate. As such, space materials must be fire-retardant and thermally resistant [4–6]. This way, if in the unlikely case, a fire does break out, and the materials of and inside the spacecraft do not propagate the flame.

Space dust is another serious challenge for space exploration [7]. During extravehicular explorations of the lunar and Martian surfaces, dust may deposit onto the astronaut's suits. This dust may later be dislodged once the astronaut has returned to the cabin. Inhalation of lunar dust has been shown to cause chronic respiratory problems, and there is good reason to suspect the same would occur for Martian dust. The constant bombardment by cosmic rays coupled with the presence of iron in lunar and Martian regolith results in the dust becoming electrostatically charged which exacerbates the challenge of space dust since it is statically attracted to virtually all materials. It is also highly abrasive so once deposited onto a given material, space dust is extremely damaging. Finally, the deposition of dust onto solar panels significantly diminishes solar power conversion—a vital energy source in space. Currently, NASA is attempting to save the InSight Mars rover since its solar panels have been coated in dust, and without its solar panels being operational, the rover cannot continue to function. It is critical to develop materials/technologies that can either actively remove/repel the dust or to develop materials where the dust cannot adhere to the surface, virtually sliding off the material's surfaces. These kinds of materials/technologies are so-called self-cleaning [8–10]. Much work is being and has been undertaken over the past decade to understand how these materials and technologies can be utilised in spacecraft and the exploration of space to mitigate the risks and challenges of space dust.

Beyond low-Earth orbit, electromagnetic radiation interferes with and causes damage to equipment [11, 12]. In particular, electromagnetic interference (EMI) can interfere with spacecraft navigation systems. The enormity of space means functional navigation systems are paramount. EMI also poses the threat to astronauts' health of radiation sickness and a high risk of cancer. Electromagnetic radiation is ubiquitous in space due to the uniformity of the cosmic microwave background; it cannot be avoided. Electromagnetic radiation can be shielded using electron-dense materials. Many materials are electron-dense, such as metals. However, the cost and amount of rocket fuel required for space travel are significant. Therefore, metal-based EMI shields are not practical or feasible. Additionally, there are technical issues with metallic-based EMI shields stemming from the reflection-dominated shielding mechanism. The challenge then becomes understanding how effective absorption-dominated EMI shielding can be achieved without significantly adding mass to the spacecraft. Several lightweight materials and nanomaterial composites have now been identified for their exceptional EMI shielding properties, and researchers are now expanding their knowledge of how these materials can be improved and integrated into spacecraft engineering [13, 14].

In space, spacecraft come in intermittent exposure to the sun's heat, affecting the material's dimensional stability. During thermal cycling, materials expand against high temperatures (Steller light) and contract at low temperatures (Shadows). This thermal abruption comprises the mechanical performance, generating cracks in structures and leading to delamination. In addition, upon leaving and re-entering Earth incredibly, high temperatures are generated due to the friction of Earth's atmosphere on the spacecraft body as it moves through the atmosphere at high speeds. Spacecraft must therefore be capable of withstanding and dissipating thermal energy. But in addition to managing the extreme thermal energy gradients impinged upon the spacecraft

during travel, vast amounts of thermal energy are also produced from inside the spacecraft. The densely packed electrical systems, as well as the astronauts themselves, produce thermal energy. Without managing this thermal energy in some fashion, the temperature inside the spacecraft cabin would become unbearable to occupy. Thermal energy must therefore be managed both internally and externally, concerning the spacecraft cabin. This classically involved the combination of highly thermally conductive and highly thermally insulating materials to prohibit the penetration of thermal energy into the spacecraft cabin and refrigeration systems for managing thermal energy on the inside of the spacecraft. Recently, however, the boom in nanomaterials has enabled much progress in exploring and understanding how thermal energy in spacecraft can be better controlled, dissipated and managed using advanced active and passive thermal management materials/technologies [15, 16].

In addition to the hazards and risks of space exploration, one of the largest challenges and hindrances is the cost. Without debate, the spacecraft, equipment, training and mission crew cost large sums of money. But one of the largest costs of space travel is rocket fuel. It costs around USD 10,000 kg^{-1} to reach near-Earth orbit due to the high price of rocket fuel and the immense amount of fuel required to overcome Earth's gravitational pull. Whilst this is a high price, it is but a fraction of the previous cost (USD ~ 30,000 kg^{-1}). The magnitude of this price reduction suggests it is unlikely that such a significant cost reduction will occur again sometime soon. The way to reduce the cost of space travel is therefore to reduce the mass of the spacecraft. Primarily, researchers are exploring how the weight of spacecraft can be reduced by engineering multifunctional structural composites. This field of research aims to engineer a material that can act as a structural component on the spacecraft, such as the hull, whilst also simultaneously acting as an additional component on the spacecraft, such as a battery [17]. By fulfilling two functions with a single component, the mass of the spacecraft can be reduced and therefore so too can the cost associated with space travel. Researchers are currently working intensively in this area to realise effective and reliable multifunctional structural composites.

Mono-functional properties, traditional manufacturing styles and conventional engineering materials are inadequate to negate the serious safety concerns for astronauts and the challenges posed to space missions. These concerns and challenges have limited the expanse of space exploration [18, 19]. Therefore, the focus of the scientific community has shifted towards developing hybrid technologies, multifunctional capabilities and self-repairable materials, guided by advanced computational material modelling. The scope of this review herein provides the most prestigious and latest insights into state-of-the-art emerging materials with use, or potential use, in applications for space missions [20–22]. As such, we skew the focus of our review on, but not be exclusive to, emerging materials for space applications found in the literature within the last 5 years.

2 Self-healing materials for space application

Space exploration and interplanetary colonisation require long-lasting, extremely reliable and self-adaptable space materials which can repair autonomously if spacecraft systems and structures are damaged. Conventionally engineered materials used in space applications are vulnerable to mechanical, thermal, UV and chemical damage. The inherent degradation of spacecraft components through repeated use must be addressed. For example, electrical wiring is prone to a degradation phenomenon known as electrical treeing, and carbon fibre composites are prone to failure due to repeated mechanical loads. The distal positioning of spacecraft from Earth means that repairing damaged components is challenging. These damaging factors limit the lifespan of spacecraft components. As a result, spare parts must be carried by spacecraft, occupying storage space and adding to the mass of the payload. However, self-healing materials can repair damage autonomously, extending the lifespan and reducing the payload by omitting the need for spare parts. Developing self-healing materials for spacecraft can lead to the realisation of safe and reliable space structures (space suits, optical surfaces, liquid-propellant containers and protective coatings), opening the possibility for longer-duration missions [23, 24]. Spacecraft must withstand high radiation levels, extreme temperatures and the vacuum of space [25]. But in particular, spacecraft should be equipped to recover from high-velocity impacts from sharp foreign objects and micro-meteoroids as these impacts may lead to catastrophic failures or gas leaks, endangering the life of astronauts [26]. Implementing self-healing materials in spacecraft engineering would improve the safety, reliability and associated cost of space missions by mitigating the risks to astronauts posed by the challenging environment of space and by reducing the necessity for part replacement [27].

2.1 Self-healing polymers

Self-healing polymers are categorized as either extrinsic or intrinsically self-healing. Extrinsic self-healing polymers rely on healing agents, whilst intrinsic self-healing polymers rely on the polymer's chemical functionality and molecular structure, as shown in Fig. 1. Healing agents are polymerizable compounds, loaded inside microcapsules or microvascular networks (containment vessels) and embedded throughout the polymer matrix. Once damage occurs, the containment vessels rupture and release the contents into the damaged area. Polymerization of these contents allows

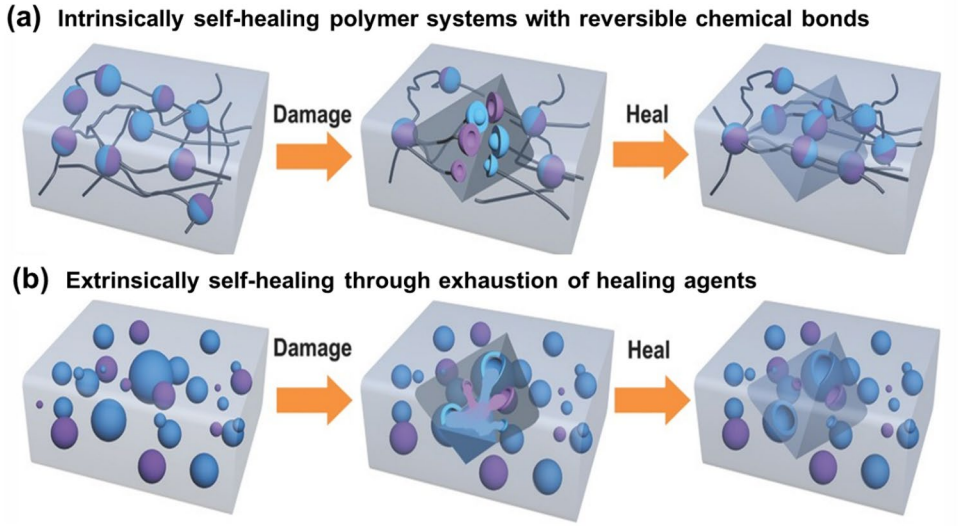

Fig. 1 Schematic illustration of **a** intrinsically and **b** extrinsically self-healing polymer systems. Reproduced with permission [31] Copyright 2017, *Advanced Energy Materials*

for self-healing of the damaged area [28]. Epoxy resins have many applications in space; naturally, the development of self-healing epoxy materials is in high demand. Guo et al. [29] reported a self-healing epoxy coating that could readily be applied to composites as a protective polymer coating. The authors synthesised SiO_2 microcapsules impregnated with epoxy resin and a UV photo-initiator. Damage to the epoxy coating breaks the SiO_2 microcapsules releasing the epoxy resin and photo-initiator into the damaged area whilst the omnipresent UV radiation in space triggers the polymerization of the resin. Generally, coatings are sensitive to humidity and delaminate due to surface condensation. However, sensors may assist in responding and recovering at right time [30].

UV radiation in space requires that the microcapsules for healing agents be composed of a non-UV penetrable material, like metal or metalloid oxides. Otherwise, healing agents are prone to polymerizing before damage occurs, inhibiting their healing capability. Li et al. [32] reported the synthesis of hybrid SiO_2/ZnO microcapsules loaded with UV-curable epoxy resin to yield a self-healing epoxy that could maintain its self-healing capability even after 21 days of UV radiation. Furthering this work, the same team then explored coating SiO_2 microcapsules with polydopamine to improve the dispersibility of the healing agents throughout the epoxy matrix [33]. Similarly, Zhu et al. [34] reported acrylate microcapsules decorated with TiO_2 nanoparticles and impregnated with epoxy/siloxane monomers. Here, the TiO_2 prevents the core resin from polymerizing by blocking UV radiation from reaching the resin. However, once damage occurs, the acrylate microcapsules become exposed to UV radiation which causes the degradation of the acrylate polymer. This further breaks down the microcapsules, improving the release of the resin core.

Another example of the applications for self-healing epoxies in space is mitigating the damage to wire insulation housing caused by electrical treeing. Gao et al. [35] produced SiO_2 microcapsule healing agents containing a photo-curable epoxy resin and embedded them in the electrical wiring housing polymer matrix. Additionally, the authors also incorporated electroluminescent TiO_2 nanoparticles throughout the matrix. Once electrical treeing occurs, the microcapsules rupture, releasing the photo-curable epoxy resin. When an electrical field passes through the wiring, this causes the electroluminescent nanoparticles to fluoresce, thereby curing the healant epoxy resin and healing the electrical treeing damaged area.

The above-discussed examples of self-healing polymer resins are examples of two-part extrinsic self-healing polymers; they are well known for being capable of self-healing, but are infamously slow, often taking several hours to recover. In space, if the debris travelling at high-speed puncture the walls of a spacecraft, this may lead to the rapid and catastrophic ejection of oxygen from the cabin. Therefore, a situation like a breach of the space shuttle's wall requires immediate and rapid self-healing to stop the catastrophic loss of oxygen. White et al. [36] developed a rapid self-healing two-stage polymer system that progresses from liquid to gel and then gels to a polymer. In the first stage, damage triggers reactive monomers (gel catalyst and gelator initiator) to create the semi-solid scaffold, largely healing the damaged area within minutes. In the second stage, complete polymerization and crosslinking occur within 3 h to restore the mass loss and spatial void completely.

Zavada et al. [2] also proposed a high-speed self-healing method for space materials. As depicted in Fig. 2, this method relies on laminating an oxygen-stimulated resin between two structurally supportive layers. The oxygen-rich

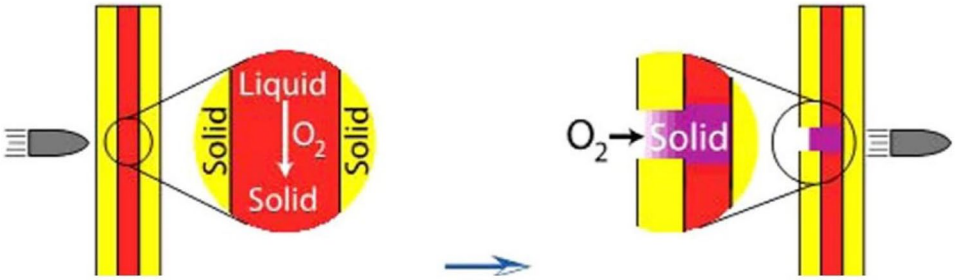

Fig. 2 Rapid self-healing of a punctured plate where oxygen immediately initiates reaction as soon as projectile penetrates the plate. Reproduced with permission [2] Copyright year, publisher, American Chemical Society, 2015

environment inside the space shuttle acts as an initiator for the self-healing mechanism. During the breach of the space shuttle's wall, the resin begins to flow into the damaged area. Immediately, the oxygen from inside the spacecraft cabin promotes radical-mediated polymerization and starts filling the gap created by debris. As the oxygen-stimulated polymerization proceeds, the viscosity of the reactive healant liquid increases until the damaged area is filled with solid polymer, acting like a plug for the breached area. In summary, oxygen-stimulated self-healing approaches are suitable for self-healing space materials owing to the speed at which they can heal damaged areas. Because the oxygen in the cabin environment immediately reacts with the healant resin, oxygen-stimulated self-healing polymer resins can self-heal within seconds, compared to conventional self-healing methods which take several hours to heal.

In addition to physical damage, self-healing polymers can enhance spacecraft longevity by mitigating damage from atomic oxygen (AO). Many polymers used in space applications, including polyimides, are susceptible to AO-induced degradation. This causes nano/micro-cracking which then propagates into complete macroscale cracking. Lei et al. [37] reported the synthesis of an extrinsically self-healing polyimide/polysiloxane blend. Oxidation of this film converts the polysiloxane into SiO_2 at the sight of AO damage. As such, this forms an epidermal film of SiO_2. The SiO_2 serves two purposes: (1) SiO_2 is resistant to oxidation, forming a protective layer for the bulk material, and (2) SiO_2 forms a solid material that can fill the damaged area.

Aromatic polyamides are often the first choice for insulating materials used in space. Kapton (a patented commercialized polyimide) is used for wire insulation due to its excellent thermal stability and mechanical and electrical properties. However, aromatic polyamides become more rigid with age and become vulnerable to crack propagation due to orbital debris, friction, heat and electrical treeing. For example, during the take-off of the Space Shuttle mission STS-93, an electrical short was the cause of losing primary engine control. Inflatable structures such as habitats also risk damage and puncture from orbital debris, micro-meteoroids and sensitive equipment. In such places, self-healing inflatable structures are a high priority to avoid the loss of atmospheric gas.

Jolley et al. [38] developed self-healing materials based on low-melt polyimide, polyurea and polyurethane chemistry, to deliver self-healing properties to electrical wires in space using three different approaches. They demonstrated the self-healing of a polyimide film by showing the closure of the cut, 10 mm in thickness, over time. One approach uses low-melt, high-performance polyimide films that exhibit flow at relatively low temperatures. When cut or damaged and at temperatures above 23 °C, the low-melt polyimide is free to flow into the damaged area, filling the void and healing the damaged area. The second approach is based on classical extrinsic self-healing polymer technology where microcapsules containing self-healing agents, when broken, release a healant to fill the generated crack or cut. Additionally, microcapsules containing volatile solvents are prepared using in situ polymerization or intra-facial techniques. These capsules are then integrated into polyamides and used for electrical wire housing. When a wire is cut or damaged, the capsule breaks and releases the volatile solvent, partially dissolving the polyamide to fill the cut or damaged area. After some time, the solvent evaporates, leaving behind a solid polymer. The developed low-melt polyimide polymer has a melting temperature range from 70 to 300 °C.

Intrinsic self-healing polymers rely on the polymers' chemical functionality and molecular structure; ergo, their healing mechanisms rely on chain mobility. This decreases at low temperatures; hence, intrinsic self-healing polymers find fewer applications in space. Nevertheless, there are reported intrinsic self-healing polymers that can effectively function in the colder temperatures of space. For example, Wang et al. [39] reported an AO-resistant intrinsic self-healing supramolecular polymer. The authors realised a siloxane polymer functionalized with hydrogen bonding 2-ureido-4-pyrimidone. The amine and ketone, functional groups on the 2-ureido-4-pyrimidone, allowed for intrinsic hydrogen bonding–based self-healing. At the same time, the siloxane component of the polymer allowed for the formation of a protective epidermal SiO_2 coating upon oxidation. Once cracks formed in this polymer due to AO degradation, SiO_2 formed over the damaged area, protecting the bulk of the polymer from further damage. At the same time, the intrinsic self-healing functionality meant the bulk polymer material could heal any cracks that

may have propagated because of the initial AO-induced cracking. The intrinsic self-healing was initiated at temperatures as low as 80 °C.

Both extrinsic and intrinsic self-healing polymers have their limitations. In the case of extrinsic self-healing polymers, they are limited by the capability only to heal once. For example, suppose cracks or punctures occur in a spacecraft structure due to the impact of micro-meteoroids; the self-healing microcapsules, impregnated into the spacecraft structure, break and heal the gap or damaged area. If a second impact occurs in the same region, the healants have already been consumed during the healing process for the first impact and are thus one-time healing limited. Future research is required to understand how this limitation can be overcome. In the case of intrinsic self-healing polymers, they are limited to only healing small cracks. For instance, if micro-meteoroids strike the surface of a spacecraft structure and generate significant gaps and global cracks, intrinsic self-healing polymers rely on the polymer chains being in close proximity to one another so that they can form supramolecular bonds. Therefore, intrinsic self-healing polymers are not useful for healing such damages. Again, future research is a necessity to overcome this limitation. However, there may be some potential in including shape memory materials in intrinsic self-healing polymers. The shape memory materials can mechanically pull the edges of the damaged area together, thereby improving the size of the damaged area an intrinsic self-healing polymer can potentially heal.

2.2 Self-healing composites

Composite technology is ubiquitous in modern spacecraft engineering. The weight:strength ratio offered by carbon fibre–reinforced polymer composites is unmatched by any other material. However, like all materials in space, composites experience extreme conditions. The immense thermal expansion and contraction, coupled with the extreme mechanical loads that spacecraft composites bear, can delaminate the polymer resin from the reinforcement fibres. Carbon fibre composites with microcapsule healing agents can recover up to 56% of their fracture toughness after 24 h of healing time. They can arrest crack formation up to 150,000 load cycles, compared to just 62,000 times in new non-self-healing composites. Hence, self-healing composites are quickly becoming a demanded technology for the space sector [28]. Embedding functional polymers into traditional composite materials can repair the damages and cracks and even recover the properties close to the original level. There are different healing mechanics based on the nature of self-healing material [40]. Recently, much excitement has grown from the prospect of using carbon nanomaterials such as carbon nanotubes (CNTs) to improve the mechanical properties of the resin matrix in carbon fibre composites. Similarly, research is now emerging in self-healing composites where CNTs are being incorporated into microvascular and microcapsular healing agents to improve the mechanical strength and robustness of the healed area. Liu et al. [41] reported the self-healing and antifouling of a composite material. They prepared composite samples using polyurethane/fluorinated polysiloxane–microcapsules–silica resin embedded with IPDI@PGMAm/GO microcapsules and nano-SiO_2 particles. The sample was cut in the radial direction to investigate the healing efficiency. The healing process was performed at 65 °C for 30 min. The results showed that the tensile strength and elongation at break improved up to 92.21% and 94.35% of the original sample, respectively. The morphology of the cut area exhibited the damage was well repaired.

Aissa et al. [42] 3D printed a two-part microvascular healing agent lattice impregnated with a ruthenium-based catalyst (Grubb's catalyst), CNTs and a polymerizable epoxy monomer. Damage to the composite ruptured the healing agent lattice, releasing the constituents into the damaged area. The composite could self-heal at temperatures as low as −15 °C in as little as 100 min, and in less than a minute at temperatures surpassing 40 °C. A similar approach, only using microcapsules instead of a microvascular network, was reported by Zamal et al. [3]. Impressively, the inclusion of CNTs into the healing agents allowed the composite to regain 97% of its mechanical fracture strength compared to just 39% for the CNT-free self-healing composite.

Intrinsic self-healing composites are also possible. Feng and Li [43] reported a carbon fibre composite where the epoxy resin could undergo dynamic covalent bond exchange through transesterification. The resin was composed of a thermoset polyethene-imide (PEI) and a diglycidyl 1,2-cyclohexane-dicarboxylate (DCN) curing agent. The PEI's tertiary amines acted as an internal catalyst for the transesterification between the peptide and ester bonds formed between reacted PEI and DCN. The system was capable of undergoing bond exchange at room temperature. It could regain up to 85% of its mechanical properties after 64 h of healing at room temperature after the damage occurred. Putnam-Neeb et al. [44] studied the self-healing of soft and stiff epoxy thermosets. The authors introduced dynamic bonds by incorporating silanolate-functionalized oligosiloxane into a soft crosslinker (1,4-butanediol diglycidyl ether) and a stiff crosslinker (diglycidyl ether bisphenol A), at 40 wt%, 60 wt% or 80 wt% concentrations. The results showed that out of these epoxy crosslinking ratios, a workable epoxy network could not be formulated. Among these ratios, 60 wt% appeared as the optimised ratio for the study. The authors found that the self-healing efficiency of a soft epoxy thermoset was better than stiff epoxy thermoset which exhibited ~ 90% tensile strength of the virgin sample. The soft epoxy network at 60 wt% increased the T_g value

(11 °C), tensile strength (3.9 MPa) and strain at break (29%). Another researcher, Fang Chen, along with his team, developed thermally conductive glass fibre–reinforced epoxy composite intrinsic self-healing capability [45]. They used a dual-coating method using DMY-functionalized hexagonal boron nitride (h-BN) micro-sheets and Diels–Alder (DA) reversible bond–crosslinked epoxy to investigate the thermal, mechanical and self-healing properties. The DA reversible bond–crosslinked epoxy networks played the role of a matrix with recovery capabilities. However, the results indicated that the built-in DA bonds restored the tensile strength of 70 ~ 85% and the thermal conductivity of 62 ~ 89% which makes it a suitable material for electrical insulation applications. However, both properties were already compromised whilst introducing the Teflon implant in the pre-damaged sample. The artificial crack did not allow heat conductivity through the thickness of the sample during the curing of a sample. Generally, such self-healing by reversible covalent bonding requires external sources like heat, pH and light. However, Liu et al. [46] introduced a different approach to the self-healing of a composite substrate at room temperature by introducing borate-based dynamic covalent bonds. They developed crosslinked polymer (CLP) boroxine/waterborne polyurethane composite leather coating which starts the self-healing process immediately after being exposed to water. The results indicated that the self-healing efficiency increased with an increase of CLP-boroxine. It reached up to 93.6% after 4 h of self-healing at room temperature when CLP-boroxine is 15%. CLP-boroxine has molecular chain flexibility; however, the rapid self-healing rate is concurrently due to hydrogen bonding between waterborne polyurethane and CLP-boroxine.

Self-healing hollow fibre composites are one of the most exciting prospects to emerge from self-healing composites. Madara et al. [47] reported that hollow glass fibres, impregnated with healing agents, could be woven into carbon fibre weaves to fabricate carbon fibre/glass fibre composites. The hollow glass fibres would break upon the damage, supplying the polymerizable epoxy resin to the damaged area. The appeal of this approach is as follows: using glass fibres as the vessels for the polymerizable resin serves both as healing agents and reinforcements for the composite. In addition, because the glass fibres are so long, they can store a large amount of resin, allowing for the healing of large areas of damage. This approach yielded a composite that could regain up to 92% of its mechanical strength, an exceptionally high healing efficiency for a self-healing composite where the resin is not yet infused with CNTs. Incorporating materials like CNTs or graphene into the resin is a naturally logical procession for this technology with tremendous prospects. A similar approach was followed by Sun and his research team [48]. They investigated the self-healing performance of the composite materials embedded with metal/polymer microcapsules. They used hollow shells filled with a low molecular weight chemical. The metal microcapsules were fabricated through a chemical plating technique. They proposed self-lubricating mechanics with microcapsules filled with isocyanate. As the load was applied to the composite material, the microcapsules broke and released isocyanate to lubricate the area under friction. The results indicated that the 10 wt% polymer microcapsules decreased the friction by over 80% under a range of loads, whereas 10 wt% of metal microcapsules decreased by less than 10%. Traditionally, weak shells result in poor strength of composites. However, metal microcapsules showed higher strength of composite materials compared to polymer microcapsules.

2.3 Self-healing metals and ceramics

Metals and ceramic materials play a critical role in spacecraft engineering. Any self-healing mechanism requires either molecular or atomic mobility. This mobility (dislocation movement) in polycrystalline structures can be varied easily by grain boundary, whereas these variations in dislocation motion and grain boundary are sensitive to the temperature. Zhao et al. [49] studied the interaction mechanism between grain boundaries and dislocation in nano polycrystalline composites. The results indicated that the rise in temperature increases the velocity of dislocation motion. They observed that high temperature decreases energy consumption and the change of energy. The temperature needed for metals and ceramics flow is much greater than that for polymers. Ergo, self-healing metals and ceramics are non-trivial. Nevertheless, several creative solutions to this challenge have been reported. Metal–matrix composites (MMCs) offer an innovative way of achieving self-healing metallic materials. MMCs are composed of a bulk solid metallic phase blended with a low-melt eutectic phase. Upon heating, the eutectic phase melts and flows into the damaged area. Fisher et al. [50] reported a self-healing antimony/copper alloy blended with a zinc eutectic phase. After the damage to the MMC occurred, heating allowed zinc to flow into the damaged area. Next, in the presence of oxygen, zinc could react to form ZnO. ZnO has a higher melting point than pure zinc, and as such, the reaction of zinc into ZnO results in a solid deposition of ZnO into the damaged area. Another exciting capability for MMCs is to dope them with shape memory alloy (SMA) wires. Fisher et al. [51] demonstrated that including SMA wires in MMCs can increase the size of the damaged area that can be healed. The healing mechanism proceeds as follows: as the MMC is heated, the actuation of the SMA wires is triggered, effectively pulling the edges of the damaged area towards one another. Simultaneously, the eutectic phase is melted and flows into the damaged area. The limitation of the MMCs' self-healing mechanism is that the edges of the damaged area must be

proximal. This limitation is somewhat overcome by pulling these edges together with SMA wires. Other SMA materials, for example nickel–titanium and Heusler alloys, may have also shape memory effects. Nambiar and his team [52] studied the microstructure and mechanical properties of annealed quinary Ni-Mn-Sn-Fe-In Heusler alloys. They increased the compressive strength of the alloy from 380 to 850 MPa and its toughness 48 times by adding Fe content to the alloy. Song et al. [53] used SMA fibre for crack recovery of engineering cementitious composite (ECC). ECC is a ductile material; however, adding nickel–titanium alloy fibres may improve the toughness and crack recovery performance. The results showed that adding 0.6% and 0.9% and nickel–titanium improved 72.91% of four-point flexural strength and 19.3% of compressive strength, respectively. The alloy fibres enabled the shape memory effect after 45 ℃ heat treatment and decreased the crack width of the sample.

Typically, self-healing metals require thermal energy input to facilitate the self-healing process. However, this is not always plausible or possible in specific spacecraft components. Wiring and circuitry, for example, cannot be heated to the temperatures required to trigger MMC self-healing—the polymeric insulation housing would be destroyed. Wu et al. [54] reported a conductive metallic nano clay that could be extruded or 3D printed into wires or circuits, capable of exhibiting self-healing properties with pressure. The authors took commercially available synthetic nano clay (Laponite) and replaced the water component with a 75:25 gallium:indium alloy. The inclusion of Laponite provided the clay with high viscosity, so the material does not flow without pressure. At the same time, the conductive liquid metal/clay mixture was a shear-thinning non-Newtonian fluid; upon applying pressure, the material's viscosity would decrease, allowing the liquid metal to flow into the damaged area. Embedding this clay into self-healing polymers holds the potential for completely self-healing wiring or circuitry. One another approach is to improve the strength of metals through high-temperature welding and forming. Wang et al. [55] investigated the influence of hot forming on the mechanical properties of ultra-high-strength steels. The results indicated that the hot-forming process improved the tensile strength and elongation of steel samples by 75% and 50%, respectively, than that without hot-forming samples. The hot-forming process increased the hardness from the base metal to the HAZ, on average 2.6 times greater than that of without hot-forming.

Another interesting self-healing metal material that does not require heating to trigger the self-healing process is layered nickel/aluminium composites [56]. Nickel and aluminium react in a highly exothermic reaction; however, the activation energy is sufficiently high that the material is stable under normal conditions. When sufficient energy to overcome the activation energy is input into the system, the exothermic reaction between nickel and aluminium is triggered. The temperatures generated by this reaction can reach up to 1500 °C, whilst the melting point of this alloy is only 1090 °C. The reaction activation energy is low enough that high-energy impacts, like micrometeoroid impacts, can trigger the reaction. The material can effectively weld its damaged area in response to a high-energy impact. Whilst this material can only heal nano-sized cracks, it can heal cracks up to 500 nm in less than 1 ms. This avenue of research is still highly novel. Ergo, the prospects of this kind of technology still hold great potential.

Self-healing ceramics reported in the literature rely on chemical reactions to self-heal, as opposed to phase changes, as ceramics are used in spacecraft as thermally resistant materials. Hence, it would be unfavourable for self-healing ceramic materials to heal via temperature-dependent phase changes for space applications. However, this poses a challenge to developing a self-healing ceramic material. Nakao and Abe [57] realised an alumina/silicon carbide ceramic that can self-heal in an oxygen-rich environment at temperatures above 1130 °C in response to AO damage. At these temperatures, silicon carbide reacts with oxygen to form SiO_2. In comparison to silicon carbide, SiO_2 is less dense. Therefore, the oxidation of silicon carbide into SiO_2 causes a significant volume expansion, allowing the damaged area to seal. At the same time, SiO_2 is resistant to oxidation, so its formation also protects the ceramic from further AO-induced damage. Tong et al. [58] prepared modified ceramic matrix composites with a new type of Cu-Si alloy at relatively low temperatures. The introduction of Cu with free Si not only improved the mechanical properties but also reacted with Si and avoided residual silicon in the matrix. Cu-Si-modified ceramic matrix composites reached the fracture toughness value of 13.55 ± 2.91 MPa $m^{-\frac{1}{2}}$ and flexural strength value of 258.75 ± 29.01 MPa.

Another self-healing ceramic was reported by Shao et al. [59] in 2019. In this work, the authors coated ZrO_2 fibres with a WSi_2-$MoSi_2$-Si-SiB_6 ceramic to yield an AO damage–incurred self-healing ceramic. SiB_6 reacts with oxygen to form SiO_2 and B_2O_3. Next, these two compounds react to form borosilicate glass. At temperatures as low as 570 °C, the borosilicate glass melts to flow into the damaged area. The temperature at which the SiB_6 oxidizes onsets is 500 °C. Hence, the ceramic is resistant to damage from AO at temperatures below 500 °C. Once this temperature is reached, only a 70 °C increase is required before the material starts healing. As mentioned, self-healing ceramics is still highly challenging. Further research and testing are necessary for this area, yet the prevalence of ceramics in spacecraft engineering undeniably makes progress here would be highly fruitful for spacecraft engineering.

3 Fire and heat-resistant materials for space applications

Fire is an imminent threat to astronauts on space missions or even to future colonies that may 1 day inhabit the surface of Mars—the tight and enclosed living conditions rich with oxygen, coupled with the lack of a safe and easy escape route, amplify the risk of fire to life. The primary source of fire in space is expected to be electrical and heating overloads, aerosol leaks, energetic experiment failures and the ignition of waste. The first reported fire fatality of an astronaut was in 1961 at the Soviet Union space program during an endurance experiment in an oxygen-rich (50% oxygen) low-pressure altitude chamber. A discarded alcohol cotton ball used to clean the astronaut Valentin Vasiliyevich Bondarenko's body fell on a hot plate and caught fire. He tried to cover the flame with his woollen coat, which caught fire in the oxygen-rich atmosphere. In 1967, a cabin fire during the launch rehearsal of NASA's Apollo 1 mission was also fatal, losing all three astronauts in the vehicle [60]. A fire outbreak in space would be one of the most dangerous occurrences possible for astronauts. Ergo, it is of utmost importance to ensure the risk of fire in space is highly mitigated. This involves ensuring that materials used in and onboard spacecraft are fire-resistant wherever possible.

The behaviour and character of fire in a microgravity environment differ, compared to being in Earth's atmosphere. From the early stages of space travel, a detailed study has been conducted on the dangers of fire in spacecraft. Real-time automated experiments in space and simulated experiments on Earth are undertaken to understand fire in microgravity better. All materials sent to space are tested for flammability. The results help create advanced spaceships, satellites and international space station (ISS) expansion modules with optimum safer materials.

Fire-retardant materials are enormously applicable in space missions. Be it in the design of the space shuttles, satellites, space suits, interplanetary vehicles or the ISS, fire-retardant materials can be found virtually in every component or technology bound for space. A complete list of materials used for fire resistance and thermal management in space is outlined in Table 1. Figure 3 also illustrates where these materials can be employed. Materials used for thermal protection systems in space are equally crucial as fire-retardant materials because the first criterion for a material to be used as a thermal protection system is that it must be fire-retardant. The surface temperature of a space shuttle may reach up to 1477 °C when re-entering at a speed of ~7700 m/s. The kinetic and potential energy of the ultrasonic vehicle is converted into heat due to friction from the atmosphere. Whilst designing fire and heat-resistant objects for space applications, the target properties of ideal materials are thermal conductivity, lightweight, reusability and low cost. Mitigation of these extreme temperatures is achieved by utilising the thermal protection system (TPS) developed to apply to the aluminium body of the spacecraft. TPS is a combination of different materials discussed in our review section.

3.1 Fibre-reinforced composite materials

3.1.1 Fibres

High-temperature stable fibres are critical for TPSs for space. Carbon fibres are conventional materials from the early stages of space travel due to their thermal stability, lightweight and strength. Carbon–carbon materials' advent as a TPS commenced in the late 1950s with NASA's Apollo mission. The criteria to nominate carbon–carbon for TPS applications included its high mechanical strength at 1650 °C, large thermal gradient and low coefficient of thermal expansion [61]. Carbon–carbon composites of strong covalently bonded atoms contribute high strength that is retained at temperatures as high as 1500 °C [62]. In 2014, carbon fibre–reinforced epoxy composite material replaced conventional metal cryogenic fuel tanks. Boeing and NASA created cryogenic fuel tanks for rockets capable of withstanding extreme temperature conditions [63]. Enormous thermal loads are generated by combustion-based rocket propulsion engines. Hence, the exit cone for rocket nozzles is now made from carbon–carbon composites due to the high-temperature handling capabilities and fire retardancy of carbon–carbon composites [4]. Researchers are exploring replacing combustion-based propulsion engines with electric-based propulsion engines to reduce the thermal load [64]. But until this technology is further developed, carbon–carbon composites are invaluable for the design of rocket nozzles. Silicon carbide (SiC) fibres are another versatile material for high-temperature applications in space, such as in gas turbine engines. This material can withstand temperatures up to 1480 °C with prolonged exposure and is less susceptible to oxidation than reinforced carbon–carbon composites. The environmental resistance of SiC fibres is further enhanced when doped with boron nitride [65]. Carbon–SiC composites are used to manufacture the thrust chambers and other hot surfaces of rockets [4].

3.1.2 Space suite and insulation fabrics

After the disastrous fire in Apollo 1, modified fire-resistant A7L Block II space suits were developed and fabricated from heat and flame-resistant fabrics 'Nomex' and 'beta cloth'. Nomex is a synthetic flame-resistant meta-aramid

Table 1 List of materials used in space for fire resistance and thermal management

Material	Type	Composition (reference only)	Used as	Properties
Reinforced carbon–carbon [4, 78]	Fibre	Graphite fabric and phenolic resin	Thermal protection system (TPS) Cryogenic fuel tank	Reproducible strength at 1650 °C Large thermal gradient Low coefficient of thermal expansion
Silicon carbide fibre [4]		Silicon	Thermal protection system (TPS) Cryogenic fuel tank	Thermal stability
Alumina fibre [86]		Aluminium	Heat shield for re-entry vehicle	Thermal stability
Borosilicate fibre [65]		Boron nitride/silicon carbide		
Nomex (fabric) [87]	Fabric	Meta-aramid fabric	The outer layer of the space suite	Synthetic flame-resistant fabric
Beta cloth (fabric) [66]		Silica fibre Teflon	The outer layer of the space suite Shower enclosure in Skylab	Flame-resistant fabric
Ortho fabric (fabric) [67]		Gore-Tex Kevlar Nomex	Space suite	Fire-resistant, waterproof, breathable
Orion Crew Survival System (OCSS) [67]		Not revealed	Space suite	Fire-resistant, breathable
Mylar (polymer film, coating) [88]	Film, coating	Polyethene terephthalate	Multi-layer insulation (MLI) systems	Thermal insulator
Silica aerogel [69]	Solid		Cryogenic fuel tank insulators	Fire retardancy, low thermal conductivity, low shrinkage at high temperature
Silica tiles [89]	Tile	Silica Water	To cover spaceship	Faster heat dissipation
Silica alumina tiles [89]		Silica alumina	To cover spaceship	Faster heat dissipation
Reinforced carbon–carbon tiles [75]		Carbon fibre, epoxy	To cover spaceship	Faster heat dissipation
Silicon carbide coating [75]	Coating	Silicon	Protective layer	Better coefficient of thermal expansion Protects from oxidation
Ceramic coating [76]	Coating	–	Protective layer	Protects from erosion
Silicon elastomer [77]	Ablator	Silicon	Protective layer	Formation of char at high temperature
Ceramic Chartek 59 [77]	Ablator	Brazed steel Fibre glass Phenolic epoxy resin	Protective layer	Formation of char at high temperature
The Phenolic-Impregnated Carbon Ablator (PICA, PICA-X, PICA-3) [90]	Ablator coating	–	Heat shield	High-temperature stability
Reaction-cured glass (RCG) [89]	Ablator coating	Tetraboron silicide borosilicate glass	Heat shield	High-temperature stability
Toughened Unipiece Fibrous Insulation (TUFI) [89]	Ablator coating	Borosilicate glass Silica-boride Molybdenum disilicide	Heat shield	Thermal cycling effect Reduced catalytic heating
High-efficiency tantalum-based composite (HETC) [91]	Ablator coating	Tantalum disilicide	High-temperature operations	High-temperature stability

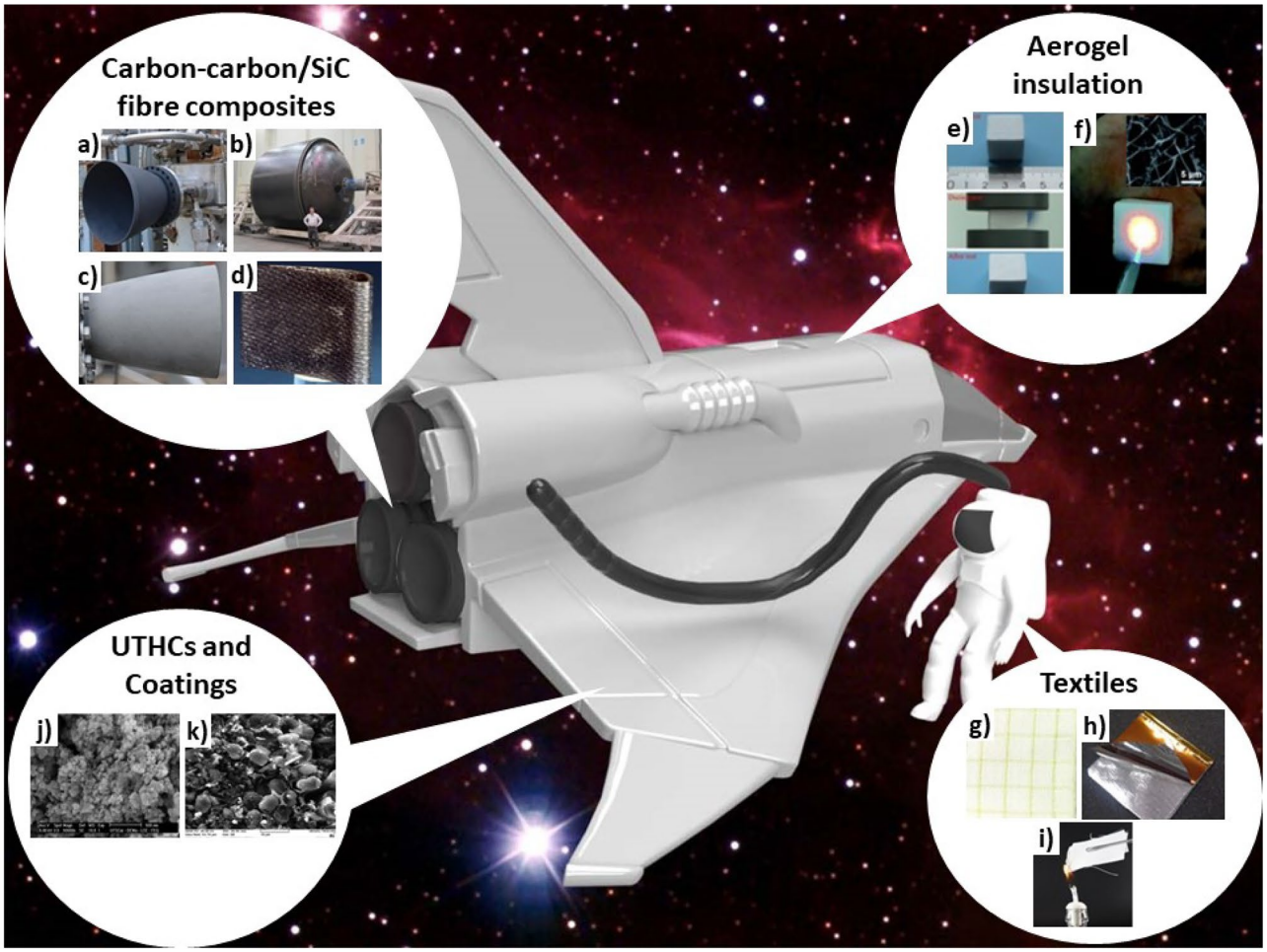

Fig. 3 Fire/thermally resistant materials are used for spacecraft and astronaut suit manufacturing. **a** Carbon–carbon composite fuel propellant nozzle [4]. **b** Carbon–carbon composite cryogenic fuel tank [78]. **c** SiC/carbon–carbon composite fuel propellant nozzle [4]. **d** BN-doped SiC/carbon–carbon composite TPS [65]. **e** Aluminium/silica aerogel as a mechanically robust thermal insulator [70]. **f** Elastic and robust super thermally insulative silica nanofibrous aerogel [71]. **g** Ortho-fabric for fire-resistant astronaut suits [79]. **h** MLI TPS used on European Space Agency's Rosetta spacecraft [80]. **i** Beta cloth for fire-resistant astronaut suits [81]. **j** Scanning electron micrograph of ZrO_2/C ultra-high-temperature ceramic used as TPS for spacecraft components [74]. **k** Scanning electron micrograph of SiC coating on carbon fibre used to thermally protect carbon fibre composites [75]. Copyright, publisher 2016, Gardner Business Media Inc [81], 2022, MDPI [83], 2020, Royal Society of Chemistry [84], 2019, Elsevier [88], 2014, Elsevier [89]

fabric used for thermal micrometeoroid garments and provides better protection for extravehicular activities in space. Beta cloth is a fireproof fabric made from silica fibre, giving incombustible characteristics to space suits [66]. Beta cloth is a woven fabric consisting of twisted ultrafine glass filaments coated with Teflon (polytetrafluoroethylene (PTFE)). Beta cloth and Nomex were used for space suits and spaceships in Apollo, Skylab (the first space station) and many other space shuttle missions during the 1970s and 1980s. In later years of the space mission, a better material known as 'Ortho-fabric' (a Gore-Tex, Kevlar and Nomex blend) was used to cover the outer layer of the space suite. In 2019, NASA announced a next-generation Orion Crew Survival System (OCSS) suit with improved fire resistance; the constituent materials are unknown [67].

The use of fire-resistant fabrics is not restrained solely to space suits but is also widely used for multi-layer insulation (MLI) systems in space. The thermal balance system, which maintains the temperature in ISS and other space modules, is an MLI system comprised of a highly reflective blanket made of aluminized Mylar and Dacron. Mylar (biaxially oriented polyethene terephthalate) was first developed by NASA in 1964. Ozdemir et al. [68] observed that graphene nanoplatelets (GNPs) were used as an effective thermal barrier for PET in the presence of ethylene methyl acrylate (EMA) copolymer. The latest in this technology is Woven Thermal Protection System (WTPS). Controlled placement of fibres in a 3D woven thermal system with different compositions and spacing is possible to optimise variable re-entry conditions and related altered temperatures [5].

This will accommodate NASA's current and future needs for space travel and re-entry requirements. Heatshield for Extreme Entry Environment Technology (HEEET) project, which develops WTPS, aims to safely re-enter high-speed interplanetary probes from Venus, Saturn, Uranus, comets and asteroids with their sample return mission. HEEET TPS is a dual-thermal protection system with a carbon layer over a blended carbon phenolic yarn to manage heat load.

3.1.3 Aerogels

Thermal management in space is more than managing fire across a range of extreme temperatures. Cryogenic liquid hydrogen and liquid oxygen that fuel space shuttles must be maintained between − 235 and − 183 °C to remain liquid. Aerogels are commonly used for this action, and silica aerogel is the most popular. Aerogels are gels with gases replacing the liquid component. They are lightweight and have very low thermal conductivities. Heat transfer through this material is limited due to its ability to hinder conduction, convection and radiation. Gaseous heat conduction is low due to its nanoporous structure, limiting the collision of gaseous molecules that cause heat transfer. Solid heat conduction is lower as the lattice vibration around the equilibrium position causes lower thermal conductivity in low-density silica aerogels [69]. Flexible composite sheets made from fibre-reinforced aerogels, glued with epoxy, are used for thermal management in cryogenic applications. Silica aerogels are prone to shrinkage and have weak mechanical properties, which is a limitation for its application and can be improved by multifibre composites [6]. An alumina-silica aerogel composite manufactured by direct sol immersion gel and supercritical fluid drying method has shown very low shrinkage at temperatures as high as 1200–1500 °C without any deformation [70]. Recently synthesised binary network–structured silica nanofibrous aerogels (BSAs) possess ultra-low thermal conductivity (21.96 mW m^{-1} K^{-1}), fire retardancy and thermal insulation performance [71]. No heat dissipates through a 20-mm-thick material of BSA when one side is heated at ~ 1000 °C due to the effect of porous aerogels. This highly fire-retardant thermal insulator was synthesised using nanofibrous silica aerogels with binary network silica aerogels.

3.1.4 Ultra-high-temperature ceramics

Ultra-high-temperature ceramics (UHTCs) are borides, carbides and nitrides of transition elements such as hafnium, zirconium, tantalum and titanium. They have high melting points, high thermal conductivity and thermal shock resistance [72]. They are stable above 2000 °C and are used as TPSs in spacecraft. Strong covalent bonding and high negative free energies of formation are responsible for high melting points and thermal stability [73]. UHTC material was used in Slender Hypersonic Aero-thermodynamic Research Probe (SHARP) (SHARP-B1 and SHARP-B2) projects in the 1990s. Fibre-reinforced UHTCs are suitable for sharp leading edges of re-entry vehicles 29. Manufacturing UHTCs was a challenge confronted earlier due to the requirement of high temperature and pressure to hot press UHTCs. Recent researchers successfully synthesise UHTCs using microwave-assisted carbothermal reduction methods [74].

3.2 Films, coatings and ablative materials

Carbon fibre composites and fabrics are extensively used to cover the exterior of spaceships to protect them from high heat during re-entry. Carbon oxidizes rapidly during this event at higher temperatures resulting in composite degradation, and coating helps to avoid this scenario. Silicon carbide-coated carbon–carbon composites show an improved coefficient of thermal expansion [75]. Similarly, a smooth ceramic coating is applied on silicon carbide ceramic materials used in spacecraft engines via the plasma spray physical vapour deposition method. This ceramic coating prevents the composite from erosion in high combustion environments [76]. NASA's Space Transportation System (STS) used fire-retardant latex paint to protect the space shuttle's external tank from ultraviolet radiation for its first two missions (STS-1 and STS-2).

Reaction-cured glass (RCG) is a coating applied on silica-based tiles used for thermal protection systems. RCG consists of tetraboron silicide borosilicate glass that provides stability up to 1650 °C for the tiles. Toughened Unipiece Fibrous Insulation (TUFI) is a surface treatment of silica tile using borosilicate glass, silica-boride and molybdenum disilicide. A simulated test with a thin layer of RCG over a TUFI tile improved thermal shock and thermal cycling effect and reduced catalytic heating. High-Efficiency Tantalum-based Composite (HETC) is used for higher-temperature operations using tantalum disilicide.

The use of ablative materials to protect vehicles during re-entry has been observed from the early stages of manned space missions. Ablative materials protect vehicles from high thermal loads during re-entry, but are not reusable, as they burn to form char—they dissipate heat by surface radiation, and the char layer provides high-temperature insulation. Project Gemini is NASA's second human space flight where they used a paste-like silicone elastomer as ablative material, which hardens when poured into a honeycomb form [77]. The Apollo vehicles command module was coated with an ablative material composed of a fibre glass honeycomb shell filled with phenolic epoxy resin. This, during re-entry, was charred to form a protective layer. The technology evolved into commercially produced 'Chartek 59', the world's first

intumescent epoxy coating. It expands when exposed to heat and burns off to dissipate heat, protecting the underlying material. NASA also developed a flexible, low-density ablative material that demonstrates equal property benefits as its rigid counterpart and retains its flexibility even after charring. The phenolic-impregnated carbon ablator (PICA) heat shield was initially developed by NASA and later improved and used by SpaceX (PICA-X) for their dragon capsule outfit. PICA-X and its next-generation PICA-3 is a lightweight high-temperature stability ablator that is stable up to 2500 °C.

3.3 Recent development in fire-resistant materials for space applications

Continued research and development of new reusable fire-retardant materials are constantly improving for spaceships and space stations. Recently, in the James Webb telescope launch of December 2021, NASA used a sunshield made of five thin layers of Kapton, each layer coated with aluminium and two sun-facing layers coated with doped silicon coatings to protect the space telescope from the sun's heat [82]. Also, the Parker Solar Probe spacecraft's heat shield, which is expected to reach the sun's corona by 2025, is another example of progress in the field of fire-resistant and thermally stable materials for space. Made of thick carbon foam sandwiched between two superheated carbon–carbon composite sheets and coated with ceramic paint, this shield reflects the sun's energy and protects the probe from high temperatures [83]. However, the most recent advancement in fire-resistant materials focuses on foreign planet-based stations and landing pads. Landing pads experience some of the highest mechanical and thermal loads of any component associated with a space mission. In search of materials to build NASA's permanent spacecraft landing pads on the lunar surface, researchers from Kennedy Space Center have performed fire testing on materials such as sintered basalt rock pavers and carbon fibre blankets filled with lunar regolith simulant materials [84]. The results will be used to design landing pad concepts for future lunar missions. Simultaneously, a student collaborative team tested a reusable 3D-printed launch and landing pad using materials found on the moon [85].

4 Thermal management in space

Spacecraft travelling from Earth to space undergoes severe thermal loads. In addition, spacecraft themselves generate large amounts of thermal energy. Thermal energy is produced from continually increasing heat loads from expanded avionic functionality, microprocessors and complex electrical architectures [92]. After 10 years of operation in low-Earth orbit, a spacecraft will undergo ~ 10,000 thermal cycles, with temperatures ranging from −100 to over 120 °C [93]. Hence, it is critical to have an efficient thermal management system for long space flights to maintain optimal conditions for the crew and equipment and to protect the spacecraft structure. As is the case for most challenges encompassed in space, thermal energy management can be addressed in two distinct fashions: actively or passively. Active solutions or technologies involve the input of energy, whilst passive ones do not. Each has benefits and cons; however, interestingly, these technologies do not come at the expense of one another. In other words, it is reasonably simple to engineer materials and design spacecraft to exhibit both active and passive thermal management technologies. A testimony to the demand for effective thermal management in space is the THOR project. THOR is pursuing the next generation of thermal protection systems for thermal management in space, exploring both active and passive means. Additionally, THOR is also exploring how other factors such as the entering velocity, trajectory, shape and size of the spacecraft contribute to thermal loads [94]. The THOR project is funded by the European Union's FP7 program and is a collaborative project between eight European organizations (industries, research centres and universities) and the Japan Aerospace Exploration Agency.

4.1 Active thermal control system, materials and their processing

Generally, an active thermal control system (ATCS) comprises three main components: one acquires heat, the other transports it and the third rejects the heat into space [95]. Thermally conductive fluids are commonly utilised to transport the heat from the acquisition component to be rejected into space. This kind of thermal management system is time honoured—the general engineering concept is not dissimilar to that which manages the large amounts of thermal energy produced in the internal combustion engines of cars. ATCSs are effective; however, they come with the trade-off of high energy consumption. For this reason, ATCSs are now typically only considered for large-scale space vehicles. Still, the efficacy of these systems speaks for itself. The question, therefore, shifts to how can we, through the design of inspired materials, improve thermal management technologies. A major area where materials can aid in spacecraft ATCSs is at the interface between heat-producing components and a heat-dissipating device. Thermal interface materials (TIMs) physically fill the gap between such components so that thermal energy can be more effectively transferred to the heat-dissipating device [96]. For example, electronic circuitry is a large producer of both thermal energy and structural complex. It is difficult to produce a heat-dissipating device that can effectively interface with electronic circuits. Here, foam

TIMs can effectively interface the circuitry with a heat-dissipating device, enhancing the thermal energy transfer and reducing the thermal energy radiance back into the spacecraft. Figure 4 summarises the way in which TIMs are used to dissipate and mitigate thermal energy.

TIMs can be classified into many groups, such as polymer-based composites, solders and other materials. Among them, composites with epoxy, silicone, poly(methyl methacrylate) (PMMA) and poly(vinyl alcohol) (PVA)-based polymers are the most widely used matrices due to their good adaptability to versatile solid interfaces. Generally, polymers have low thermal conductivity, but adding highly thermally conductive fillers such as ceramics, carbon materials and metals, can improve overall composite thermal conductivity in the range of 1–10 W m^{-1} K^{-1}. Graphene is a promising thermally conductive filler material for polymer-based TIMs [97]. This study used graphene and copper nanoparticles to investigate the thermal conductivity of hybrid epoxy composites. The study found that the high thermal conductivity of about 13.5 ± 1.6 W m^{-1} K^{-1} was achieved by using 40 wt% of graphene and 35 wt% of copper nanoparticles. Also, the thermal conductivity of composites with a moderate graphene concentration of $f_g = 15$ wt% exhibits a rapid increase as the loading of copper nanoparticles approaches $f_{Cu} = 40$ wt%. In contrast, in composites with a high graphene concentration, $f_g = 40$ wt%, the thermal conductivity increases linearly with the addition of copper nanoparticles.

To achieve a highly thermally conductive polymer composite TIM, a high filler loading must be achieved (up to 90 wt%). This allows for a good thermal conductive path inside the polymer matrix, increasing thermal conductivity [101, 102]. Fillers are mainly prepared by the liquid exfoliation process, including chemically modified exfoliation for graphene oxide and functionalised h-BN nanosheets and direct sonication of pristine built materials in solvents. Table 2 summarises the reported thermal properties of composites with different hybrid fillers, which revealed *synergistic* effects. For better comparison, the data are primarily shown for polymeric composites with various quasi-2D fillers, e.g. graphene and h-BN.

Recently, TIMs have also been explored for cooling highly thermally loaded surfaces of spacecraft by using the

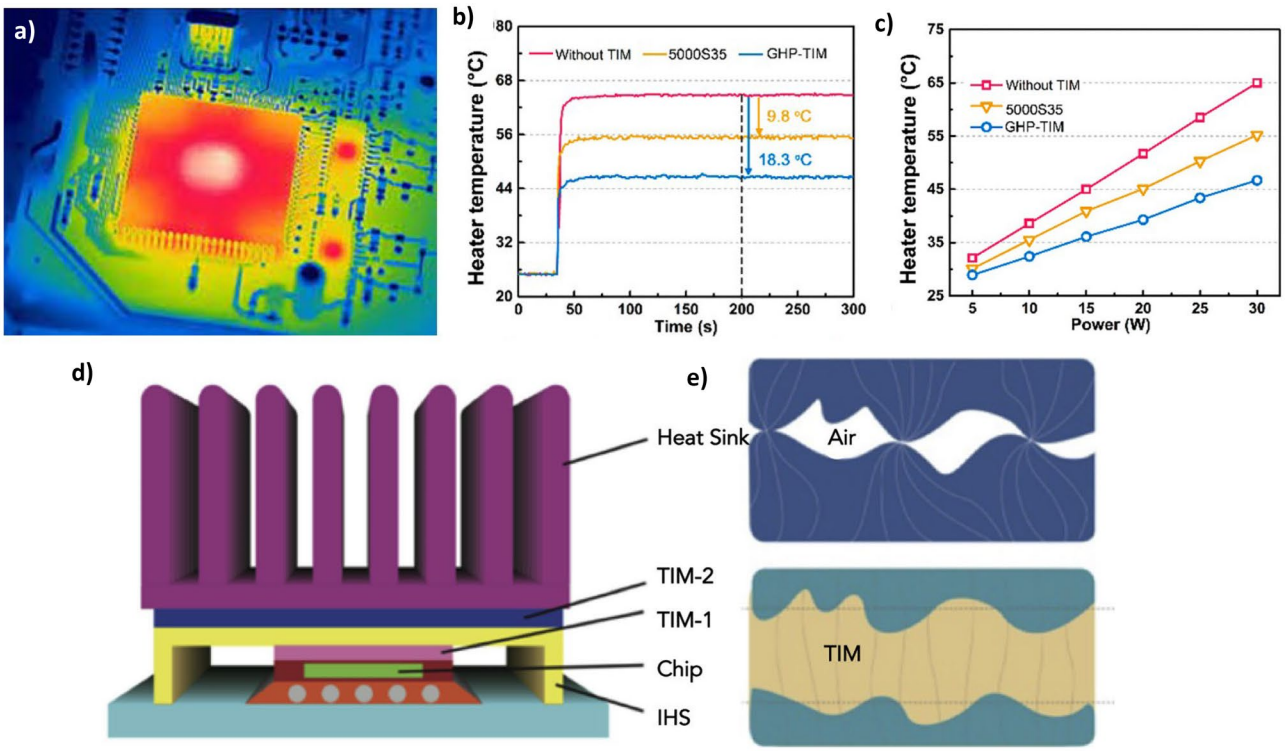

Fig. 4 Role of TIMs in thermal management. **a** Infrared photograph demonstrating computer chip generating thermal energy [98]. **b**, **c** Demonstrating heat dissipation of commercially available TIM (5000S35) and graphene hybrid paper TIM when applied to the ceramic heating plate [99]. **d** Illustration of the use of TIMs to manage chip thermal energy [100]. **e** Schematic of a TIM: An interface without TIM (top) shows conjunct heat transfer due to limited solid–solid contact, opposed to an interface with TIM (bottom) which has enhanced solid–solid contact [100]. Copyright, publisher 2019, American Chemical Society [112], 2019, Elsevier [113]

Table 2 Thermal conductivity of composites with hybrid fillers

Filler type	Thermal conductivity	Filler %	Matrix	Refs
GVP/Cu-NP	13.5 ± 1.6	40/35	Epoxy	[103]
GNS/MWCNY (silver functionalised)	12.3	20 vol%	PVA	[104]
GNP/h-BN	4.7	15/2 vol%	Epoxy	[105]
GNP/Al_2O_3/MgO	3.1	15/2 vol%	PC/ABS	[104]
CNTs grown on the GNP	2.4	20 wt%	Epoxy	[106]
GNP/MWCNT	1.8	20/1.5 wt%	PA	[107]
Ag NWs/GNP (functionalized)	1.4	18/2 wt%	PC	[108]
GNP-decorated Al_2O_3	1.4	12 wt%	Epoxy	[109]
GNP/h-BN (nanosheet)	1.0	6.8/1.6 wt%	Epoxy	[110]
GNP/h-BN	0.9	20/1.5 wt%	PA6	[107]
GNP/Ni	0.7	5.0/8 wt%	PS	[111]
GNP/MgO	0.5	30 wt%	PVDF	[112]
MgO/GNP (coated)	0.4	7 wt%	Epoxy	[113]
GNP/MWCNT	0.3	0.9/0.1 wt%	Epoxy	[114]
GO/MWCNT	4.4	49.64/0.36 wt%	Epoxy	[112]
h-BN (vertically aligned)/SiC	5.8	40 wt%	Epoxy	[115]
h-BN/MWCNT	1.7	50/1 wt%	PPS	[116]
MWCNT/Cu	0.6	15/40 wt%	Epoxy	[117]

sandwich-TPS method. This involves sandwiching a porous ceramic foam TIM between two carbon fibre composites and passing a coolant through the ceramic foam. Ortona et al. [16] described this sandwich-structured composite as shown in Fig. 5. The THOR project has used this sandwich-TPS concept to actively cool a highly loaded surface. The foam is highly porous, allowing for the passage of coolant to highly loaded areas, thereby reducing the temperature. In another research, Gallego and Klett [118] developed a highly thermally conductive carbon foam at Oak Ridge National Laboratory which does not need the conventional blowing or stabilisation steps. It rapidly reduces the temperature against high load which is highly desirable for power electronics. The results found that comparatively, carbon foam reduces the required volume of cooling fluid and is an efficient thermal management system.

4.2 Passive thermal management systems

Passive thermal control systems are generally preferred for spacecraft as they do not involve moving parts or power consumption, and there is no possibility of any component failure. Other key factors to adopt passive thermal control systems are reliability, cost and simplicity. Advanced thermally conductive materials are examples of passive thermal management technologies. These materials manage thermal

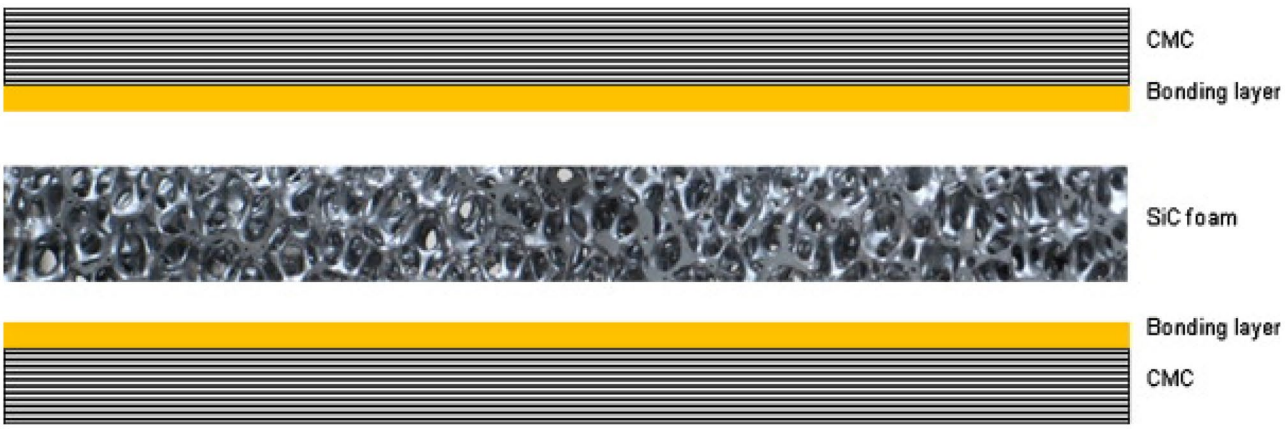

Fig. 5 Sandwich structured composites. Reproduced with permission [96] Copyright 2011, *Journal of European Ceramic Society*

energy on spacecraft by either directing or rejecting thermal energy as an intrinsic property of the material. The thermal transport of typical carbon–carbon (C–C) composites can be complex due to the heterogeneous structure of most C–C composites. This ultimately makes typical C–C composites inappropriate materials for managing thermal energy. However, C–C materials with atypical thermal conductivities are much more promising as passive thermal management technologies. Composites with highly oriented graphitic fibres, matrices or a combination of both (i.e. vapour-grown carbon fibres and matrix or mesophase pitch–based carbon fibres) exhibit high anisotropic thermal conductivities, effectively directionally transporting thermal energy through the material. The general range of conductive fibres is 10–20 W m^{-1} K^{-1}; however, the thermal conductivity of pitch-based carbon fibres is reported up to 600 W m^{-1} K^{-1}. Reimer et al. [119] investigated the benefit of using a highly thermally conductive CMC for the leading edge of hypersonic vehicles. The results confirm that the high conductivity of carbon–pitch fibre composites is a promising material for passive thermal management.

Passive thermal management can also be achieved with textiles to yield garments that help mitigate the build-up of thermal energy, improving the comfort for thermally burdening clothing and suits. Fan et al. [120] demonstrated that 3D orthogonal woven fabrics can facilitate one-way water transport for human body moisture thermal management. Although this technology is yet to be employed in space suits, it holds the potential to enable longer and more ergonomic spacewalks. Nanofluid technology is also a recent area of investigation with promising results for thermal control systems [121]. In this technology, the nanomaterials are dispersed in a solvent facilitating thermal transport through the dispersion. Mixing techniques have been developed to guarantee no sedimentation of the metallic nanoparticles, which could harm the overall heat and mass transport. By adding 5 wt% nanoparticles, the liquid thermal conductivity can be increased by 20% [122]. Kim et al. [121] and Lee et al. [123] reported the enhancement of in-plane thermal conductivity using nanofluids, nanoribbons composed of water and copper nanoparticles with sizes around 25 nm.

Phase change materials (PCMs) are also exciting materials for passive thermal management in space. They can absorb, hold and release heat to keep the space crew comfortable. PCMs provide an interesting passive method to dissipate latent heat which natural conventions do not do by themselves [124, 125]. Such materials undergo a phase transition at a certain temperature (typically 40–50 °C). Lopez et al. [15] compared active and passive thermal management techniques on lithium-ion battery cell temperature and thermal balancing. They observed that PCMs constantly kept the cell temperature under the safety operating limit of 50 °C even under strenuous thermal conditions. Without the PCM, the temperature sharply rose to an unsafe limit of temperature of 90 °C. The authors suggested that PCMs may have applications in battery thermal management which may reduce the chance of catastrophic failure.

5 Dust mitigation: processing and fabrication

During the Apollo missions, one of the most valuable and infamous lessons learned was the challenge of lunar dust. The dust is formed from continuous high-energy impacts of micro-meteorites producing electrostatically charged and radioactive particles with jagged and sharp morphologies. The lack of liquid water on both Mars and the Moon and the lack of winds on the lunar surface prevent the particles from eroding into smoothed morphologies [126]. In the Apollo missions, the lunar dust regolith was found to abrade almost everything it came into contact with. It irritated astronauts' eyes and lungs and severely damaged equipment, posing a severe risk to astronaut safety and the mission's success [127]. Years later, the issue is understood to be even more of a health risk due to the potential for radiation poisoning. Mars is also susceptible to severe dust storms. The colonisation of Mars will inevitably rely on solar power of some sort. The deposition of dust that is difficult to remove onto solar panel arrays could be detrimental to the Martian colony's survival [128]. Currently, the issue of space dust poses one of the most serious challenges faced in interplanetary colonisation.

Dust mitigation measures can be classified into (i) active and (ii) passive. Active measures involve the physical removal of dust via the application of force [129]. Passive measures involve engineering the material's surface to be self-cleaning so that the dust cannot adhere to the surface [130, 131]. Active measures benefit from rapidly removing deposited dust, but they consume energy. Passive measures benefit from not consuming energy; however, they offer less control over decontamination. Currently, NASA is exploring both measures, and in fact, NASA has been running lunar dust challenge competitions since 2016 to develop both passive and active dust mitigation measures [132, 133].

5.1 Passive dust mitigation

Passive dust mitigation measures can be perceived as self-cleaning surfaces. Most of the currently developed self-cleaning surfaces are inspired by nature. Their unique capabilities arise largely from microscale surface roughness, for instance lotus leaves, butterfly wings, gecko feet and shark-skin [134, 135]. Inspired by this, many different surfaces have been engineered to exhibit biomimetic self-cleaning properties [136, 137]. These surfaces have found many

applications on Earth; however, they also hold great potential to mitigate the devastating effects of lunar and Martian dust on spacecraft, space equipment and astronaut health.

5.1.1 Self-cleaning coatings

Self-cleaning coatings are an attractive passive dust mitigation measure since they can be easily applied to various materials to minimise the adhesive surface forces on the coated materials. Superhydrophobic coatings are attractive passive dust mitigation measures [137]. Such coatings can be realised by combining micro-scale surface roughness with non-polar surface chemical functionality [130, 138, 139].

Fluoropolymers are well known for their chemical hydrophobicity and their chemical and thermal stability. One of the most well-known fluoropolymers is Teflon. Teflon was originally developed for space applications as a low-surface energy and thermally stable polymer. Blending nanomaterials into fluoropolymers is an effective way of achieving self-cleaning surfaces. The fluoropolymer matrix provides appropriate chemical functionality, whilst the nanomaterials increase surface micro-scale roughness. The so-called 'Lotus coating' (a self-cleaning coating currently being developed by NASA as a passive lunar and Martian dust mitigation) is an example of such a coating. It can be seen depicted in Fig. 6.

The Lotus coating is a hybrid fluoropolymer/TiO_2 composite material. The TiO_2 in the Lotus coating is in the form of nanoparticles. By doping the fluoropolymer with TiO_2 nanoparticles, the nanoscale surface roughness can be increased, leading to superhydrophobicity [131, 136, 140]. In addition, TiO_2 has well-known photocatalytic properties. In the presence of water and light irradiation, TiO_2 produces peroxides enabling photo-sterilisation. This bifunctionality of the Lotus coating makes it an appealing passive dust mitigation measure. There is, however, a limitation to the applicability of the Lotus coating. TiO_2 reflects a broad range of visible light wavelengths. This means the Lotus coating is inherently opaque white, posing an obvious issue with optically active materials/technologies. It was realised that transparent self-cleaning coatings are of dire interest to space exploration as many optically active technologies are susceptible to the effects of lunar and Martian dust; solar panels are an excellent example. Solar panels will undoubtedly play a critical role in powering space exploration and colonisation missions. If these solar panels are covered in space dust, they will cease generating power; however, if coated with a self-cleaning coating such as the Lotus coating, they would be rendered active due to the coating opacity. To solve this issue, Roslizar et al. [141] reported hot-embossed fluoropolymer films can serve as optically transparent self-cleaning surfaces. Exploring three different hot-embossing temperatures, the authors concluded 270 °C was most appropriate for producing a micro-textured film with superhydrophobic properties; temperatures greater than this (280 °C and 290 °C) lead to a loss of superhydrophobicity. The film hot embossed at a temperature of 270 °C exhibited a contact angle of 156° and demonstrated effective self-cleaning properties (see Fig. 7). Interestingly, this coating was also anti-reflective due to its unique surface topography, leading to a net increase in the power output when applied to solar panels [10, 141].

As mentioned in this review, Kapton is a highly utilised material in spacecraft engineering. Given the prevalence of

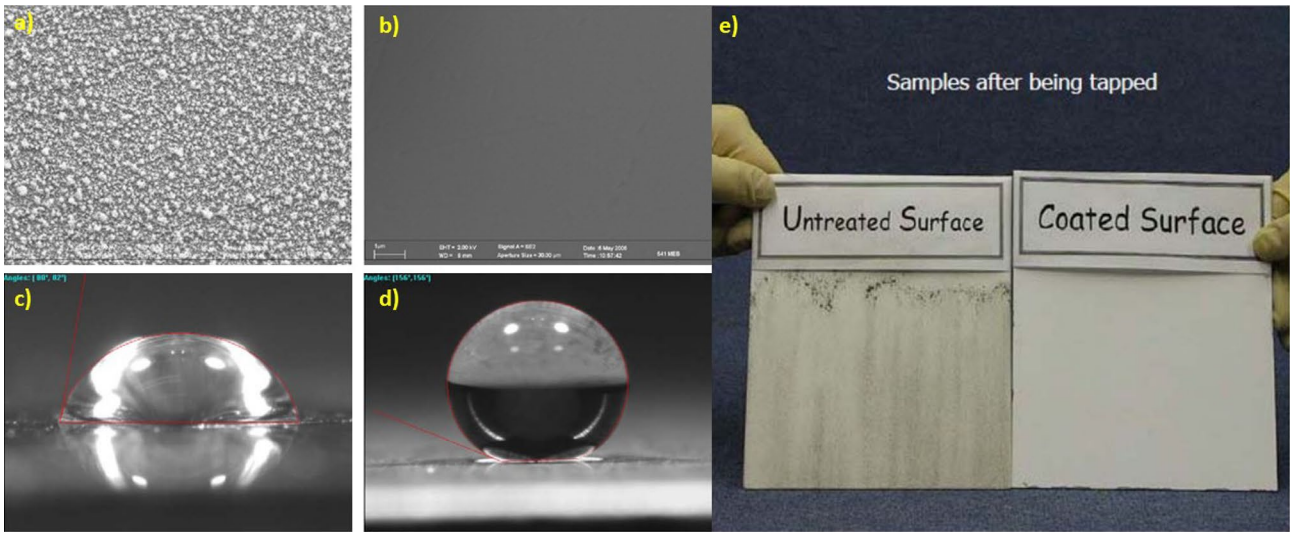

Fig. 6 **a** Depicting scanning electron microscopy image of the surface with Lotus coating. **b** Scanning electron microscopy image of surface without Lotus coating. **c** Water contact angle without Lotus coating. **d** Water contact angle with Lotus coating. **e** Demonstrating the self-cleaning properties of Lotus coating. Reproduced with permission [136] Copyright year, publisher 2010, SPIE

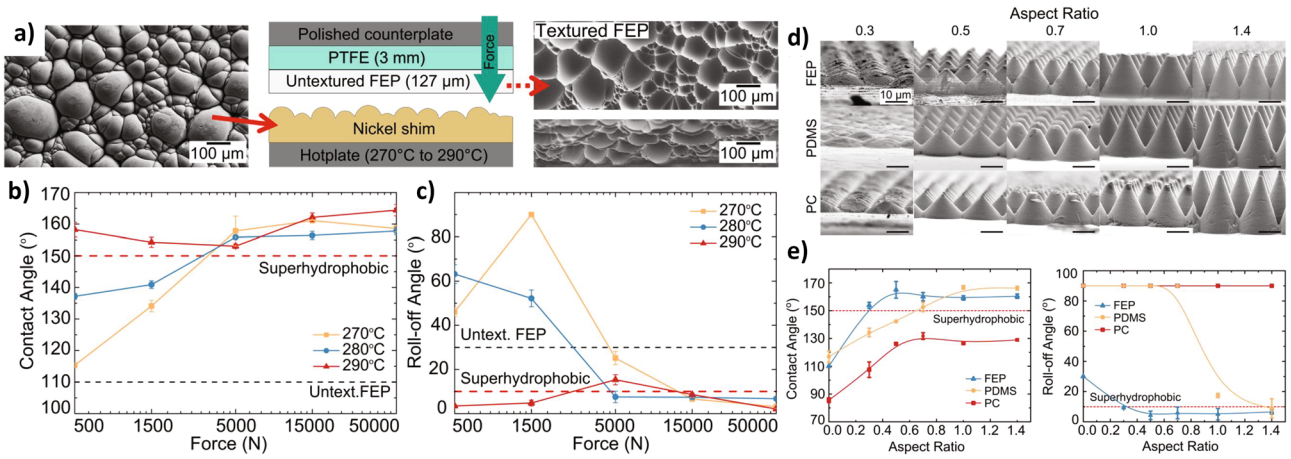

Fig. 7 **a** Schematically depicting the hot-embossing method. **b** Demonstrating the water contact angle of the hot-embossed fluoropolymer coatings. **c** Depicting the roll-off water angle for the hot-embossed fluoropolymer coatings. **d** Depicting improved surface roughness topography via the hot-embossing method. **e** Demonstrating the associated improved superhydrophobicity. Reproduced with permission [10, 141] Copyright year, publisher 2018, Elsevier, 2020, Elsevier

Kapton in spacecraft engineering, it is paramount to develop a method to endow Kapton with self-cleaning properties. Plasma ion–irradiated Kapton exhibits lower van der Waal's surface forces and electrostatic charge surface capacitance than untreated Kapton—this decreases the adhesive forces between particles and the treated Kapton; as such, self-cleaning surface Kapton can be achieved. Whilst there are no current uses of ion beam–treated Kapton in spacecraft, this approach was found to be highly effective. Ergo, as space exploration and spacecraft engineering advances, it is likely that ion beam–treated Kapton will be adopted shortly [137, 142].

5.1.2 Self-cleaning textiles

Realising self-cleaning textiles for space dust mitigation is still challenging but in high demand. It was well documented that during the Apollo missions, the lunar regolith severely abraded the astronaut's suits, posing a serious threat to the safety of the astronauts—self-cleaning textiles could mitigate this threat. Textiles fabricated from robust and low-surface energy polymers (i.e. polytetrafluoroethylene or polyvinylidene fluoride) hold potential due to their unique chemical properties. Among researchers, passive self-cleaning textiles are often considered the preferred technology due to the possibility of powerless lunar and Martian dust mitigation. Despite this, to the best of our knowledge, there have been no successful reports of passive self-cleaning textiles for the application of space dust mitigation. Since Apollo 17, there have been no manned missions intending to explore the lunar or Martian surfaces; hence, there has been no need for dust-mitigating self-cleaning textiles in space exploration. But within the last few years, the intent for such missions has been announced by NASA. Hence, despite the lack of successful reports of self-cleaning textiles for lunar and Martian dust mitigation, there is a newfound interest in the development of self-cleaning materials for space applications.

Self-cleaning textiles for terrestrial applications have been realised for almost a decade now [143, 144]. Like self-cleaning coatings, theoretically, self-cleaning textiles for terrestrial applications should be applicable for lunar and Martian dust mitigation. Furthermore, research in self-cleaning textiles for terrestrial applications has progressed to a point where researchers are now exploring multifunctional self-cleaning textiles. There may be potential in some of these emerging materials as simultaneous passive and active dust-mitigating textiles by exploring multifunctional self-cleaning and conductive textiles. Zhu et al. [145] reported superhydrophobic flexible, robust, copper nanoparticle–decorated conductive textiles. Graphene-coated textiles also show potential in this area; Shateri-Khalilabad and Yazdanshenas [146] reported superhydrophobic conductive graphene-coated cellulose textiles.

Like Lotus coatings, TiO_2-coated self-cleaning textiles also show good potential for applications in space. TiO_2 can be synthesised hydrothermally, allowing for the seeded growth of nanoparticles directly onto substrates. Besides, TiO_2 can also be combined with other dopants such as graphenaceous materials to add to the composite material functionality, achieving conductive, self-cleaning and photosterilising textiles [147, 148]. The idea of a superhydrophobic and conductive textile is an attractive premise for a multifunctional textile with both active electrodynamic shielding (EDS) protection and passive self-cleaning protection. Again, there are no current successful reports of self-cleaning textiles for applications in space to the best of our knowledge. Nevertheless, theoretically, the potential exists; therefore, this is an active field of research that holds much potential.

5.2 Active dust mitigation

Active dust mitigation technology is a desirable approach to solving the lunar and Martian dust issue. Compared to passive dust mitigation technologies, these technologies rely on power consumption. Active dust mitigation measures can be sub-classified into three categories: (1) fluidal, (2) mechanical and (3) EDS. Fluidal approaches rely on applying different fluids to transport dust particulates away from a contaminated surface. Applied fluids may be liquids, gels, foams or gases [149]. However, these approaches are energy consumptive and unfeasible. Mechanical techniques rely on mechanical work via either brushing, blowing, vibrating or ultrasonication of particulates away from a contaminated surface [150]. But similar to fluidal-based methods, these methods either are ineffective or leave the contaminated surface abraded due to the dust morphology [151].

Electrodynamic measures involve the application of an electrostatic field that levitates dust particulates off and away from a surface [150]. The most appealing active technology for dust mitigation is the use of EDSs. EDSs propagate a moving electromagnetic field parallel to the object's surface which it is shielding. This facilitates the levitation of particles off shielded surfaces and prevents the deposition of newly settling particulates [152]. EDSs can be fabricated into thin and flexible films, making them ideal for solar panel electrodynamic shielding [153]. However, the prospect of using this technology for textiles has also recently become realisable [8]. There is now exciting potential for using EDSs in many aspects of space exploration, namely EDS solar panels, spacecraft and extravehicular astronaut space suits.

5.2.1 Electrodynamic shielding

EDSs are based on the technology of electric curtains [154]. A series of spaced electrodes are fashioned into an insulating material. The system produces both standing and travelling electrical waves when applying an alternating current. This results in dust particulates levitating both perpendicularly off the EDS surface and tangentially transported away from the EDS [154–156]. Biris et al. [155] published the first paper on implementing EDSs as active lunar and Martian dust mitigation measures. The prototype consisted of a series of parallel conductive wires embedded in a polymeric film. The authors achieved over 50% cleaning efficiency with relatively low power consumption. The team conducted rigorous experimental tests to scrutinise the technology under simulated Martian environmental conditions. The results showed great promise giving much hope for the plight of EDS technology in extraterrestrial environments [157]. Furthering this research, Calle et al. [158] laminated electrodes in a dielectric polymer film to realise an EDS. The EDS was applied to several different material surfaces, including transparent solar panels and opaque metallic paint. The authors tested the technology under simulated Martian environmental conditions and demonstrated a cleaning efficiency of ~ 97%. In 2013, the team mounted solar panels, protected by EDSs, onto the outside of the International Space Station to observe the developing technology's space dust mitigation capabilities during space travel. This experiment is still in progress as the sample panels are yet to be retrieved from the International Space Station [9, 129].

EDSs are highly versatile dust mitigation measures. Aluminium electrodes laminated in a polyimide film were reported as an effective (74% removal of dust) EDS for door seals, capable of preventing space dust from penetrating bearings and mechanical door seals in spacecraft [159, 160]. Nowadays, nano-micro materials have greatly improved the functionality and efficacy of EDSs. Silver nanowire–based electrodes laminated between dielectric polymers can produce transparent EDSs, whilst silver microparticle–based electrodes yield opaque EDSs, which each showing shielding efficiencies of > 95% [152]. Even copper-based transparent EDS electrodes have been realised when the size of the electrodes is sufficiently reduced [153]. In addition, transparent EDSs can also be achieved without nanomaterials. Indium tin oxide is a conductive and transparent material that can be used to create transparent electrodes for transparent EDSs [156]. The capability of producing transparent EDSs broadens the applicability of EDSs for space applications—they can now be applied to spacecraft windows, solar panels or lenses.

But perhaps one of the most exciting works exploring EDS technology for space applications is the integration of CNT yarns into space suits [8]. In this work, the authors reported the first-ever textile EDS with the intent of producing EDS space suits. This technology has been coined "SPIcDER" (Spacesuit Integrated Carbon Nanotube Dust Ejection/Removal) system. The conductivity, mechanical properties and weavability of CNTs allowed for their use as effective textile EDS electrodes. The technology is the first of its kind and is in its infancy. Still, the preliminary investigations showed great potential for active dust-mitigating textiles, with recorded cleaning efficiencies lying between 80 and 96%. Figure 8 portrays both the photolithographic technique reported by Bernard et al. [152] and the SPIcDER technology reported by Manyapu et al. [8] and Jiang et al. [161].

6 EMI shielding and radiation protection materials

Satellite communication systems and many modern electronic systems rely on Ku band (12–18 GHz) signalling. These electromagnetic (EM) signals interfere with satellite

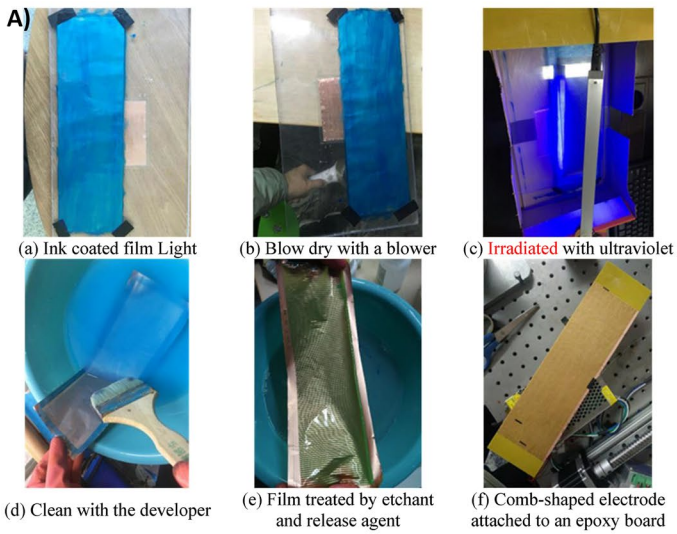

B)

Dust removal efficiency and increased efficiency of different electrode configurations.

Experimental group	Tooth (mm)	Gap(mm)	Dust removal efficiency η_0	Increased efficiency η
a	10	3	51%	28%
	5	2	85%	38.6%
b	5	2	63%	38.6%
	1	1	87%	99.1%
c	1	1	95%	99.1%
	1	1.5	32%	148.2%

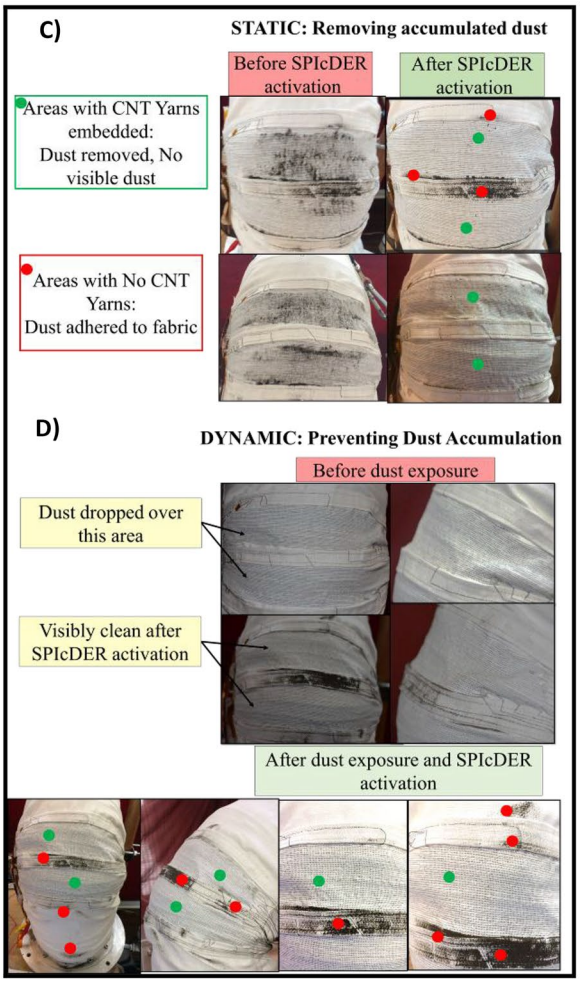

Fig. 8 **A** Depicting the photolithographic EDS fabrication technique reported by Jiang et al. [161]. **B** Demonstrating the relationship between electrode geometries and EDS performance. **C** Demonstration of SPIcDER system at removing static dust. **D** Demonstration of SPIcDER system's ability to inhibit dust deposition. Reproduced with permission [8, 161]. Copyright year, publisher 2019, Elsevier [179], 2021, Elsevier [168]

communication and are hence referred to as EMI. Without effective communications, spacecraft cannot navigate, which increases the likelihood of impacts or collisions from micrometeorites or other spacecraft. Additionally, EM radiation can be damaging to electronic systems [162]. There are several considerations for EMI shields meant for space applications: (1) The material must have low outgassing, (2) the material should be robust and stable across a wide temperature range and (3) the material should be as lightweight and low profile as possible [163]. EM radiation can be shielded mainly by three mechanisms: reflection, absorption or multiple internal reflections within the shields. Simple EMI shields can indeed be fabricated using metallic-based EMI shielding materials [164, 165]. However, metals are inherently massive, which is sub-optimal for space applications due to the high cost of rocket fuel. Shielding by reflection is also not an effective strategy as the reflected wave creates further interference with other electronic modules, causing severe EM pollution; metallic-based EMI shields are reflection EMI shielding dominant. As such, researchers are working towards developing efficient microwave absorbers by converting conductive nanofillers like CNTs, graphene, MXenes and nanoparticles into processable forms such as films, and membranes, aerogels and foams. Polymer nanocomposite shields also offer tunable electrical properties with superior processability and are considered a potential replacement for metallic shields [166–169].

6.1 Carbon-based EMI and microwave shields

Carbon-based materials are excellent candidates for EMI shielding. The combination of high electrical conductivities, lightweight, good processability, high mechanical strength and thermal/chemical stabilities equip carbon-based EMI shields with excellent properties for EMI shielding in space missions [170, 171]. Additionally, carbon-based materials

can be induced into forming multi-layered, highly porous or 3D networks with multiple interfaces which enhance the EMI shielding efficiency (EMI SE) through increased multiple internal reflections [172]. A simple and highly explored method of producing carbon-based EMI shields with multiple interfaces is through the process of freeze-drying carbon nanomaterial dispersions. Kong et al. [173] freeze-dried a CNT/reduced graphene oxide (rGO) dispersion to yield a low-density (57 mg cm^{-3}) aerogel with a high average EMI SE of 31.2 dB at a thickness of 2 mm.

Produced carbon-based aerogels can also then be impregnated with polymer resins to yield polymer composite EMI shields. Liang et al. [174] impregnated a GO/PVA aerogel with epoxy resin to yield a multifunctional composite material with an EMI SE of 51 dB, high thermal conductivity of 1.56 W m^{-1} K^{-1} and electrical conductivity of 179.2 S m^{-1} [174]. Similarly, Hu et al. [175] produced a CNT/aramid nanofibre hybrid aerogel impregnated with a fluoropolymer to yield a flexible, stretchable, hydrophobic material with an ultra-high EMI SE of ~ 45 dB at a low thickness of 200 µm. The authors concluded their work by flagging the potential for this material as an EMI shielding water-resistant textile [175]. Furthermore, Song et al. [176] showed that the approach of producing a carbon-based aerogel, followed by polymer impregnation, offers superior EMI shielding compared to simply dispersing carbon nanomaterials into polymer matrices. The authors produced an rGO/cellulose-based aerogel and, after calcination, impregnated the aerogel with PDMS. Finally, the authors produced a sample with identical rGO loading by simply dispersing the rGO sheets into PDMS. The aerogel analog held an EMI SE 3.9 times greater than the dispersed rGO sample.

As well as having good EMI shielding properties, carbon-based materials are often flame retardant, which, as detailed in the previous section, is desirable in spacecraft components. Wang et al. [177] manufactured an rGO-decorated carbon foam, derived from sugar cane, with a low density of 47 mg cm^{-3} and an EMI SE of 53 dB. The material was shown to be thermally insulative and flame retardant—such a material holds great promise for multifunctional EMI shielding spacecraft insulation.

Carbon materials can also be used as substrates which can then be further functionalized to yield a multicomponent material. Guo et al. [178] functionalized cotton fabric with WS_2/CoS_2 metal–organic framework (MOF) followed by carbonization to yield a MOF/carbon fibre composite material with an EMI SE of 51–26 dB at a thickness of 2 mm. Most notably, the material offered an absorption-dominated shielding mechanism due to the multiple reflections and impedance matching which stemmed from the multicomponent design of the composite material.

Of all the carbon-based EMI shielding materials, graphene and rGO-based materials are particularly interesting EMI shielding materials. The 2D structure, combined with the high electrical conductivity, facilitates multiple reflections of incident EM energy to improve EMI SE. Wei et al. [179] reported a method for producing polyimide films with aligned graphene sheets. The induced alignment of graphene sheets allowed for a film as thin as 60 µm to produce an EMI SE as high as 63 dB with an incredibly high tensile strength of 145 MPa and thermal conductivity of 190 W m^{-1} K^{-1}.

However, whilst graphene-based EMI shields are effective, EM radiation can be reflected to nearby surroundings due to the impedance mismatch phenomenon, creating further interference [180]. Magnetic nanoparticles (Fe, Mn, Ni and ferrites) can enhance the microwave absorption of graphene. Excess EM energy, incident on graphene's surface can interact with the free electrons and dissipate as heat energy due to ohmic and polarisation losses. The same can also be said for alternative carbon nanomaterial-based EMI shields, such as CNT-based EMI shields [181]. Hence, graphene/magnetic nanoparticle hybrids have been studied extensively for EMI shielding applications [182–184]. But regardless, graphene-based EMI shields are effective even without magnetic nanoparticles—thermally graphitised GO films exhibit nearly 20 dB EMI shielding effectiveness at low thicknesses of 8.4 µm with an absorption-dominant shielding mechanism [185, 186]. Transparent graphene-based hybrid films also offer high optical transmittance coupled with a high electrical conductivity that is of paramount use in optoelectronic devices and optical windows for space applications. Monolayer graphene has over 95% optical transparency and is the most widely used 2D material for designing optically transparent EMI shielding films [187]. Graphene–aluminium metallic networks fully encapsulated between monolayer graphene and quartz glass substrates were found to be effective optically transparent (~94%) EMI shields with shielding values of ~ 28.91 dB and 99.7% energy attenuation (Fig. 9) [13].

6.2 Polyimides for microwave absorption and EMI shielding

Given the abundant use of polyimides in spacecraft engineering, it is unsurprising that they are also explored for the production of EMI shields. Foams, of all sorts, are also valuable materials in the plight of spacecraft engineering. Their low densities and superior insulating properties make them natural candidates for insulating thermally unstable components. Given this, polyimide foams are highly applicable materials for spacecraft engineering. However, polyimides are non-conductive. To use PI foams as EMI shields, appropriate modifications must be made to boost their shielding properties [188]. Such changes involve adding conducting nanofillers into PI resin, and

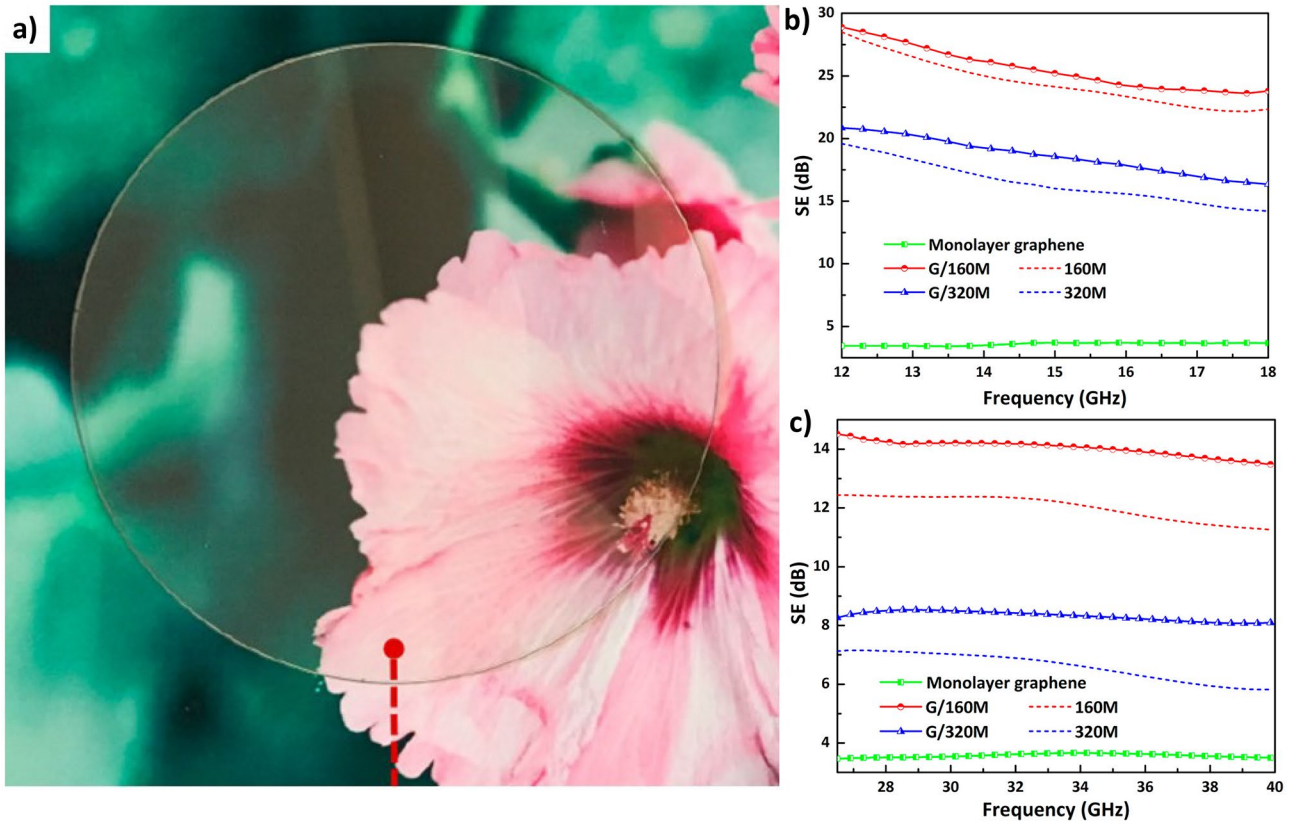

Fig. 9 Monolayer graphene-based optically transparent EMI shields. **a** Demonstration of the optical transparency of monolayer graphene-based EMI shield overlaid on top of the photograph, EMI SE of monolayer graphene, metal network and graphene hybrid films **b** at 12–18 GHz and **c** 26.5–40 GHz. Reproduced with permission [13] Copyright 2017, American Chemical Society

forming a percolating network is crucial to attaining high-performance microwave absorption and EMI shielding.

CNTs are highly conductive and EMI shielding nanofillers. However, the sp2 hybridisation of CNTs makes it difficult to disperse them throughout PI resin matrices. The dispersion of these nanofillers throughout the PI matrix is almost as crucial as the inclusion of the conductive nanofillers themselves. There are several means of improving the dispersion of CNTs throughout PI resins, such as chemical functionalisation [186], use of surfactants or incorporation of CNTs into polyamic acid followed by sequential imidization to yield a CNT/PI composite material [189]. In addition to nanofiller-doped PI foams, graphitised PI foams are attractive EMI shields with tunable porosities in large and specific surface areas, excellent mechanical properties, high thermal and chemical stability, tunable thermal conductivity and high electrical conductivities [190, 191]. These carbon foams can exhibit 24–51 dB EMI SE values depending on the thickness [192].

6.3 SiC foams for microwave absorption and EMI shielding

SiC foams are open-cell structured ceramic foams with many technological applications [193, 194]. These foams find many applications due to their low coefficient of thermal expansion, good thermal shock resistance, excellent oxidation resistance and high surface-area-to-volume ratio, making them extremely lightweight [195]. SiC foams are produced either by coating SiC powder onto foam templates or through filtration of liquid or gaseous silicon onto carbon templates. These methods allow for lightweight SiC foams with tunable porosities, making SiC foams desirable materials for EMI shielding applications in spacecraft [196]. SiC foams with low thermal conductivity can also be synthesised from biomass-derived precursor materials. SiC foams are extremely stable at high temperatures and can exhibit EMI SEs of up to 24 dB. Given the extreme temperatures experienced in space

exploration, biomass-derived SiC foams are intriguing materials for the EMI shielding of spacecraft [197].

Hybrid nanofiller/SiC foams are also highly attractive materials for EMI shielding spacecraft. Including nanofillers such as CNTs or graphene can improve the EMI shielding by increasing the electron density and even adding functionalities to SiC foams. Jiang et al. [198] freeze-cast graphene oxide–coated SiC whiskers to produce anisotropic and lightweight spongy bone-like graphene-SiC hybrid aerogels (see Fig. 10). The minimal reflection loss (RL) of hybrid aerogels reaches −47.3 dB at 10.52 GHz with an adequate absorption bandwidth of 4.7 GHz [198]. These multifunctional properties of SiC/hybrid foams make them a potential candidate for use in higher-performance EMI shielding and thermal insulation systems for space applications.

6.4 MXenes: the future of EMI shielding

Since the advent of 2D materials beyond graphene (2D-MBGs), MXenes are emerging 2D-MBG candidates for EMI shielding applications as they possess exceptional electrical conductivity (over 4600 S cm^{-1}), large specific surface area, excellent processability and low density. The surface chemistry of the MXenes can also be tuned via the addition of surface functional groups such as hydroxyls, ketones or halogens, which imparts hydrophilicity and allows for easy processing and fabrication of its hybrids/composites in aqueous solutions [14]. Naguib and co-authors [14] reported initial studies on the application of MXenes for EMI shielding. The highly flexible MXene/sodium alginate (SA) films, with nacre-like structures, exhibited 92 dB EMI SE at 45 μm thickness (> 50 dB at 2.5 μm), demonstrating the potential for MXenes as ultra-thin EMI shields [199]. The EMI SE value of this MXene-based film is one of the highest among all the synthetic materials reported to date at this thickness range. Since then, many researchers have adopted the stance that MXenes hold immense potential for EMI shielding [200–202].

$Ti_3C_2T_x$ is generally the most explored MXene for EMI shielding; however, there is some discrepancy in the literature over whether Ti_3CNT_x could potentially be superior as an EMI shield. Han et al. [203] conducted a comprehensive study where the authors synthesised all MXene structures reported in the literature and compared the various materials to one another, focusing on EMI shielding. Han and others reported $Ti_3C_2T_x$ to be superior to Ti_3CNT_x [203]. However, Iqbal et al. [204] reported several months later that their group had synthesised Ti_3CNT_x and it outperformed $Ti_3C_2T_x$ at the same thickness [204]. As alluded to by the authors, this is an anomalous result and warrants further investigation to explain the results. Like graphene-based EMI shields, the 2D structure of MXene sheets allows them to stack on top of one another and form 3D networks or multi-layered structures, facilitating multilevel shielding and increasing the EMI SE [200]. Furthermore, like graphene-based EMI shields, MXene EMI shields can be combined with polymers to produce composite materials. Wang et al. [205] doped epoxy resin with $Ti_3C_2T_x$ at a 15 wt% loading to realise a conductive material (105 S m^{-1}) with an EMI SE of 41 dB. Xu et al. [206] combined $Ti_3C_2T_x$ with polyvinyl alcohol to yield an effective EMI shield despite the material's ultra-low density of 10.9 mg cm^{-3} and the MXene loading only being 0.15 vol%. Qi et al. [207] reported a similar material but substituted hydroxyethyl cellulose for the polyvinyl alcohol. This material showed not only good EMI shielding but also good electrical cyclability, suggesting this material may have applications in EMI shielding electrodes.

Again, like graphene-based EMI shields, the alignment, layering and percolation of MXene sheets can be somewhat controlled to form unique structures that improve EMI SE through increased multiple internal reflections. Jin et al. [208] showed that by alternatively casting a $Ti_3C_2T_x$ dispersion and a PVA solution, a multi-layered material could be

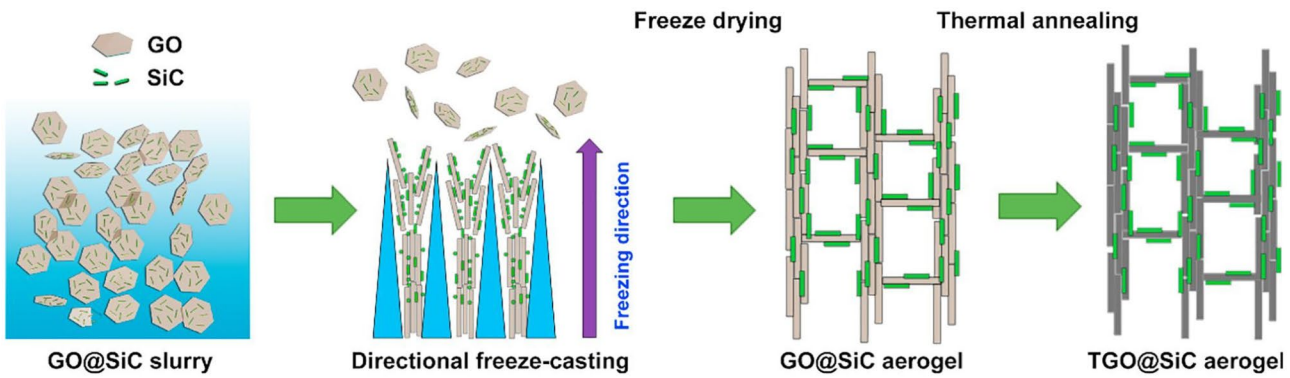

Fig. 10 Schematic representation of fabrication process for hierarchical porous, spongy bone-like graphene@SiC aerogels [198] Copyright 2018, Elsevier

yielded. At a thickness of 27 μm, the material exhibited an EMI SE of 44.4 dB, an extremely high thermal conductivity of 4.7 W m^{-1} K^{-1} and a high electrical conductivity of 716 S m^{-1}. Wu et al. [209] produced a MXene aerogel through freeze-drying and then sequentially impregnated the aerogel with PDMS to produce a lightweight, compressible, flexible and conductive material with an EMI SE of 70.5 dB [209]. Yun et al. [210] reported a method for producing nm-thick MXene films by inducing interfacial self-assembly of the sheets. This unique method reported that the thickness of the film was controllable, and this lead to a tunable EMI SE. Zhang et al. [211] also reported that the use of a doctor blade to cast a MXene dispersion can induce alignment of the MXene sheets yielding a 940-nm-thick film with an ultra-high EMI SE of 50 dB and a record-holding tensile strength of 570 MPa.

Recently, much work has been dedicated to hybridised MXene EMI shields. Typically, this involves combining MXenes with materials that have already been explored in the literature as EMI shielding materials, i.e. carbon-based EMI shielding materials and metallic-based EMI shielding materials. Liang et al. [212] used calcined natural wood as a unique carbon-based skeleton to decorate with MXene sheets. The material had a low density of 197 mg cm^{-3}, was thermally insulative and flame retardant and boasted an EMI SE of 71.3 dB [212]. Much research has also been dedicated to combining MXenes with carbon nanomaterials [213–215]. Huangfu et al. [184] combined MXene sheets with silver nanowires and aramid nanofibre to yield a flexible multifunctional material with an exceptionally high EMI SE of 80 dB at a low thickness of 50 μm, excellent flexibility, mechanical strength, electrical conductivity and the capability of joule heating [216]. Zhang et al. [217] combined MXenes with iron oxide nanoparticles yielding an EMI shield with an SE of 40 dB at a thickness of 75 μm. Cheng and co-authors [218] platted Ni onto a melamine sponge, decorated this sponge with graphene nanoplatelets and then coated it with MXene sheets and polyethylene glycol to yield a multifunctional EMI shield that also held phase change properties. Ergo, this material could be used for EMI shielding thermal management. Very recently, Guo et al. [219] reported the enhancement of an MXene/carbon aerogel by absorbing the organic dye methylene blue to yield an EMI shield with a SE of 84.3 dB at the low density of 47.1 mg cm^{-3}.

Whilst carbon and metallic materials are common materials to combine with MXenes, recently, a considerable effort has been made to explore MXene/conducting polymer hybrid EMI shields [213, 217, 220]. Intrinsically conductive polymers (ICPs) themselves hold EMI shielding properties due to the electron density. Ergo, the combination of MXenes with ICPs holds the potential for enhanced EMI shielding compared to MXene polymer composites with non-conductive polymer matrices. ICPs, such as poly(aniline), poly(pyrrole) and poly(3,4-ethylene dioxythiophene)–poly(styrene sulfonate) (PEDOT:PSS), have been widely studied. MXene/(PEDOT:PSS) composite films showcase superior conductivities of 340.5 S cm^{-1} and a maximum EMI SE value of 42.10 dB at 11.1 μm thickness with a dominant absorption shielding (see Fig. 11) [221]. Additionally, the use of ICPs enables simple functionalization of fibrous media since the ICP can be used as a binder to adhere MXene sheets to fibre surfaces. Wang et al. [222] coated polypropylene fibres with polypyrrole and MXene sheets to yield an EMI shielding textile that had an EMI SE of 90 dB at a swatch thickness of 1.3 mm. This material shows excellent potential for EMI shielding textiles [222]. These results demonstrate the higher performance EMI shielding and microwave absorption ability of hybridised MXene films. Such films are suitable for defence, military and aerospace applications. Finally, although BN is not the same as MXenes, it is a 2D-MBG in its own right and has recently shown potential for neutron radiation shielding. The abundance of neutron radiation in space is uniquely challenging for aerospace engineering. We, therefore, chose to incorporate this challenge into our review. Neutrons pass through electron clouds more readily than charged radiation. Additionally, metallic EMI shields can form radioactive isotopes when bombarded with neutron radiation, which can lead to secondary radiation sources. Hence, classical metal-based EMI shielding materials are not suited for neutron radiation shielding. Boron effectively captures thermal neutrons across a wide range, making BN an effective neutron shielding material. Concurrently, hydrogen is also effective at slowing and absorbing high-energy neutrons. Zhang et al. [223] combined BN with hydrogen-abundant ultra-high molecular weight polyethylene to realise an effective neutron shielding material. At a thickness of 3.2 mm, the material could prevent 97.2% of incident neutron radiation.

Nanocomposites and hybrid materials used for space applications must be adapted to stringent and hostile operating environments. Engineering high-performance materials that can withstand such harsh conditions require advanced manufacturing and engineering tools with high precision. Nevertheless, these space materials must also assure high reliability whilst performing intricate and sophisticated science experiments. High-performance hybrid materials, which possess multiple functionalities such as high-temperature resistance, excellent mechanical properties, ease of processability, shock/impact resistance, optical transparency and high-performance EMI shielding, are the prime requisite for designing materials for future space applications. Hence, a great deal of multidisciplinary research is being promoted to tailor these properties in hybrid materials (foams, aerogels and thin films) for use in different segments like space shuttles, satellites and mars/moon rovers.

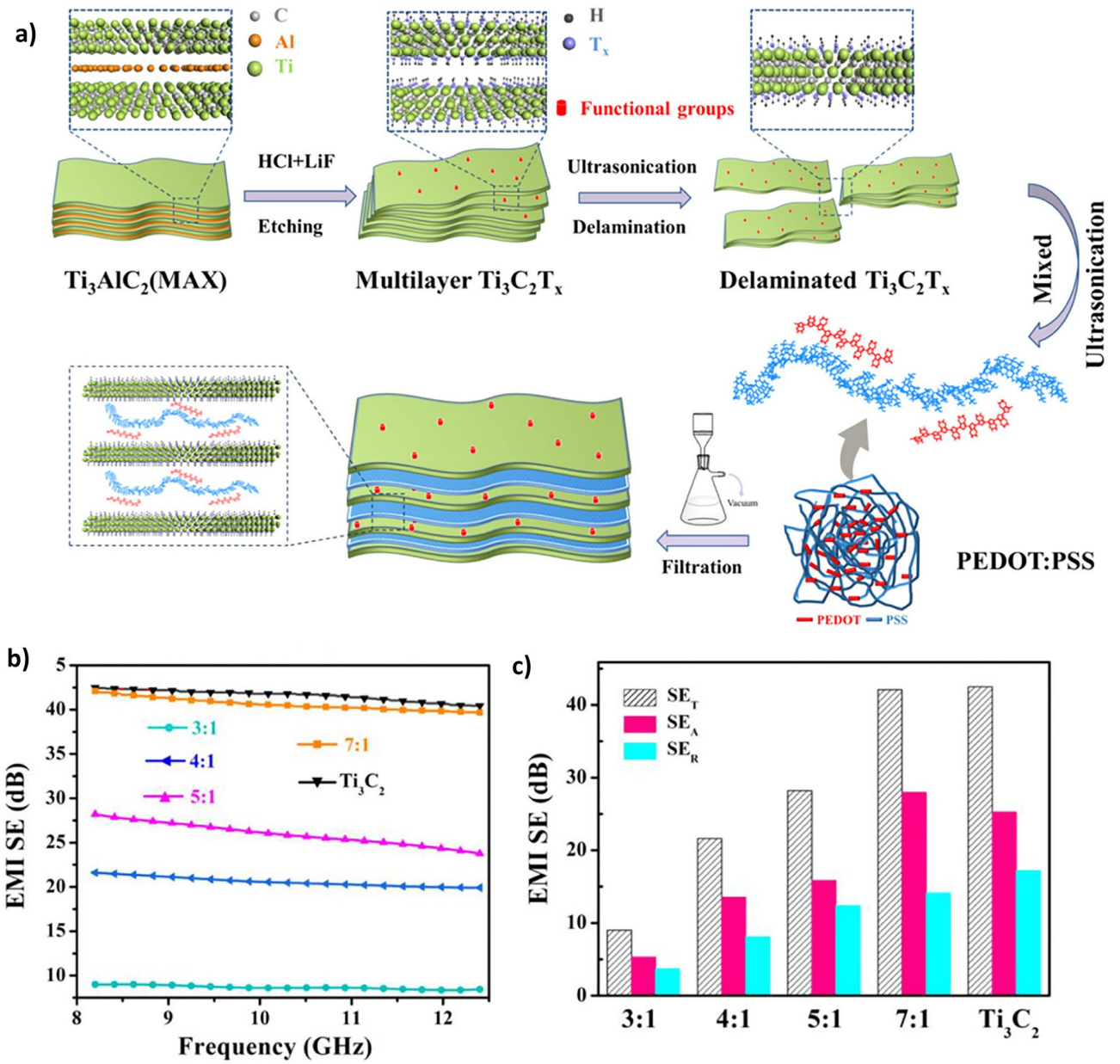

Fig. 11 **a** Schematic illustration of the assembly process for $Ti_3C_2T_x$ MXene/PEDOT:PSS composite films. **b** EMI SE of pure $Ti_3C_2T_x$ MXene film and the polymeric composite film with different ratios. **c** Total EMI SE and its absorption (SE_A) and reflection (SE_R) of pure $Ti_3C_2T_x$ MXene film and the polymeric composite film with different ratios. Reproduced with permission [221] Copyright 2018, American Chemical Society

7 Computational modelling of advanced materials for space technology

7.1 Modelling of complex materials for space applications

During the last decades, the space industry has extended computational modelling to cover complex materials across the product life cycle. Computational modelling can be utilised to design and fabricate materials with unique properties by accounting for the anisotropy of thermal expansion on space material thermomechanical properties and behaviours such as residual stress. The demand for computational modelling has also increased in space-based experimental approaches that are inherently high risks, costly or time-consuming. Further to the space applications of materials for extreme environments, computational modelling is used in lightweight structural materials, coatings, materials for electrical power generation, energy storage, power distribution, electrical machines and smart materials. Moreover, the data generated via connected objects utilising the industrial internet of things (IIoT) in the factory of future (FoF)

has created enormous opportunities to understand the root causes of material failures and address safety and quality issues whilst increasing process productivity and material reliability. Hence, there is crucial to develop innovative simulation models that predict space irreversible materials' properties and long-term response mechanisms under specific environments and operating conditions.

7.2 Areas of computational modelling in space application

The use of computational modelling spans a wide area of space applications, including concept design, modelling, design and fabrication optimisation and the analysis supporting techniques using data visualisation. Examples of national space agencies, research institutes and aerospace companies' applications cover deterministic and probabilistic models, numerical approaches, subroutine modelling and predicting various materials' multiphysics under certain operating conditions, specific lengths and time scales [224, 225]. As illustrated in Fig. 12, the nano level, represented with the quantum mechanics (QM) based on electronic structure and density functional theory (DFT), provides the most accurate and comprehensive description of material atomic structure and properties [226, 227]. Exceptionally, QM can widely predict the thermochemical properties using computational thermodynamics and electrical properties, including band gaps, optical spectra and electronic conductivity [228, 229].

This can be demonstrated in Maillard, and others' anharmonic DFT calculations of the thermodynamic properties of B-H species, where the accuracy of the analytic expressions of these functions was comparable to the NASA functions in the 200–900 K temperature range [228]. Likewise, this was demonstrated in the study of Butler and co-workers [229] and Xiang and co-workers [230], applying first-principles calculations to investigate and design materials with superior properties.

However, this high level of accuracy comes with a high computational cost, which, in turn, makes molecular mechanics (MM) and molecular dynamics (MD) highly favourable. These techniques mainly utilise numerical approaches to solve Newton's motion equations rather than finding an approximate solution for the Schrödinger wavefunction equation. Atoms and molecules' forces and potential energies are calculated using interatomic potentials or molecular force fields [231, 232]. This simple approach increases computational efficiency, providing solutions to material science challenges, including mechanical and thermomechanical properties at the microscale [233, 234]. Despite the success of MM and MD computational modelling, selecting appropriate interatomic potentials is still

Fig. 12 Key application areas of computational modelling software packages

a key challenge. Since potential energy functions have to be parametrised for all modelled chemical species whilst considering possible inter-chemical interactions, they have not been standardised. This leads to different fidelity levels depending on the system and properties modelled. Therefore, there is a need for an efficient and standardised methodology to generate reliable potential.

Whilst it is computationally infeasible to consider all functions related to atoms and molecules being modelled explicitly, many universal scaling polymeric properties, including density and composition, can be most efficiently investigated through mesoscopic models. Mesoscopic models include the pearl-necklace, the tangent hard-sphere, the bead-spring and the ellipsoidal particle [235, 236]. Moving from nanoscale, microscale and mesoscale to macroscale modelling, finite element analysis (FEA)-based computational modelling tools encompass algorithms for mechanics, heat transfer, electrical conductivity and simulation capabilities for nonlinear materials behaviour [237, 238]. FEA is beneficial in predicting different critical material properties. Furthermore, the analysis can be extended to investigate the shrinkage resulting from polymerization or crystallisation, the effect of fibre wrinkling and temperature gradients that arise in differential polymerization. The governing physics is usually modelled with thermokinetics, chemoreology, thermosets and thermoplastics, applying several constitutive material models covering linear elastic, stress–strain and viscoelastic. At the macroscale level, continuum constitutive models have proven to be well placed to predict critical properties, including deformation response and thermomechanical; however, their ability to predict damage evolution remains challenging [239]. This can be demonstrated in Nilakantan and co-workers [240] and Cao and co-workers [241] in the dual use of Kevlar-based composites in space and defence materials when using FEA modelling to investigate toughness by assessing the ballistic performance. Table 3 demonstrates some examples of computational modelling in space materials.

7.3 Future of computational modelling for materials in space

Future trends include extending all computational modelling utilisation, enabling proper handshaking between level-specific approaches and techniques and developing models that strike a balance between experimental time and length scales and computational cost and fidelity. There is also a need to link computational model outcomes with experimental measurements for validation and verification and future model development and reliability studies to ensure the integration of uncertainty from various sources into models across all levels [253, 254].

Quantum computing utilising qubit's quantum properties allows scientists to effectively consider all possible solutions, arriving at the best solution much more rapidly. Unlike conventional computers, where bits have to assume a value of either 0 or 1, a qubit can simultaneously represent 0, 1 or both values (i.e. superposition), providing solutions to problems considered impossible to be solved [255, 256]. Since the global quantum industry is maturing quickly, key players currently view quantum computing as a competitive advantage that will reshape the space industry. For instance, NASA's Quantum Artificial Intelligence Laboratory (QuAIL) hosts a 2048-qubit D-Wave 2000Q™ quantum computer to tackle optimisation problems [257]. Rigetti Computing and Airbus arranged competitions to accelerate the demonstration of a quantum computing advantage [258]. Quantum computing can be utilised in many areas, such as computational fluid dynamics (CFD) and material science [259].

Last, the adoption of an artificial intelligence (AI) approach based on machine learning (ML), for instance, will increase efficiency, enabling models to predict *materials*' properties accurately. This approach can be extended further to include 3D-generated image-based modelling for heterogeneous regions and nanofibre composite–based materials with high tortuosity and aspect ratio to precisely support computational models [260, 261]. Figure 13 summarises future trends in space computational modelling.

Table 3 Examples of the use of some computational modelling in space materials

	Levels	Modelling	Materials	Applications	References
1	Nano level	Quantum molecular dynamics	Kevlar/polyethylene	Radiation protection	[242–244]
2	Micro level	Molecular dynamics	Epoxy resins and hardener (i.e. bisphenol A, bisphenol F, triethylenetetramine)	Polymer construction material	[245–247]
			Graphene nanoplates	Lubricating oil	
			Graphene-magnesium nanocomposite	Lightweight and high strength	
3	Meso level	Hard sphere	Carbon nanotubes	Electrical conductivity/crack sensing	[248, 249]
		Empirical analysis	Graphite epoxy composite	Failure thermal cycling	
4	Macro level	Finite elemental analysis	Axial braided carbon/carbon composite	High temperature/strength	[250–252]

8 Smart composite materials

Smart composites are hybrid materials that have excellent mechanical properties and additional functionalities such as structural health monitoring, EMI shielding, energy storage and generation and self-healing. The advent of graphene, CNTs and other fillers with superior functional enhancement has greatly broadened the scope of smart composites and brought significant advancement in this area. Smart composites primarily aim to serve as structural components with additional intrinsic functionalities. This ultimately leads to a reduction in the spacecraft's weight, volume and cost. Moreover, the simplified structure enhances the lifetime and increases the functional volume. Composites like this are intrinsically smart and are in high demand for smart structures and robotics in aerospace applications.

Modification of composites, either at the interface level or throughout the matrix, commonly involves the incorporation of enhancement fillers like graphene and CNTs, to name a few [262]. Under ideal conditions, the homogeneous dispersion of nanofillers has little to no effect on the volume fraction of fibres, which are the main structural components in the composites. However, it has been observed that uniform dispersion of enhancement fillers is hard to achieve, resulting in degradation of overall structural stability. Furthermore, the effectiveness of composites functionality enhancement diminishes as the fillers tend to aggregate with higher loading during the fabrication process. Thus, there is a significant trade-off between structural and functional performance with the current technologies.

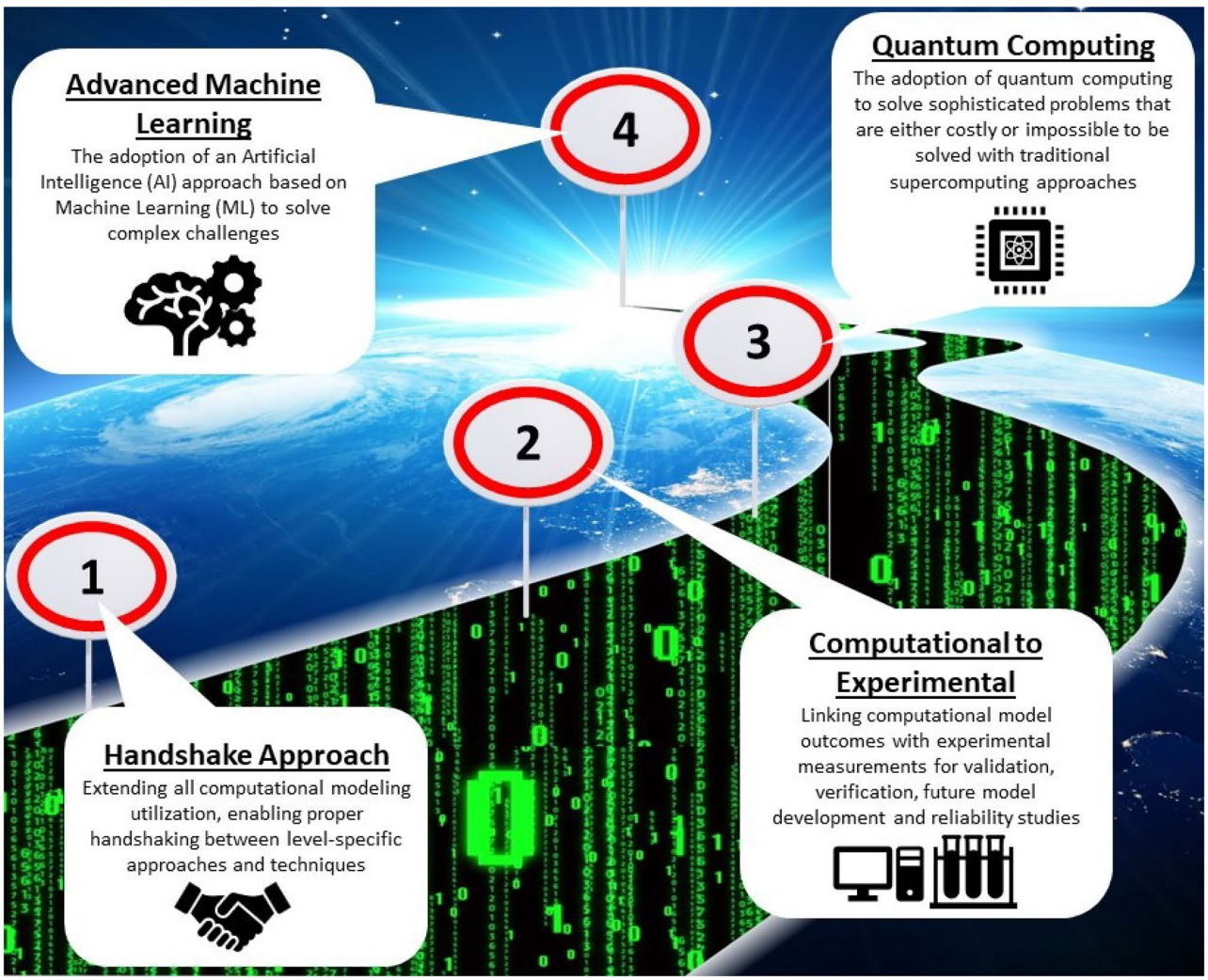

Fig. 13 Summary of future trends in space computational modelling

8.1 Energy storage structural composites

Energy storage composites are composite materials with sufficient mechanical strength to serve as structural components that also can serve as energy storage devices. Using structural components as energy-storing devices decreases the payload from battery packs, improving feasibility [263]. The realisation of energy-storing composites is still an enormous challenge, and any research in this field is still highly novel. Owing to this, few variations in fabrication approaches are found in the literature. Most cases involve directly embedded prefabricated thin-profile batteries within structural a composite. Pereira et al. [264] demonstrated that thin-film lithium-ion batteries could be integrated into carbon fibre composite to produce structural batteries. The fabricated structural battery achieved minimal charge/discharge deviation from pristine cells and the capability to withstand up to 50% of the pristine carbon fibre–reinforced polymer composites (CFRPCs) [264]. Another work also proposed the concept of structurally integrated lithium-ion batteries. The battery is encapsulated inside structural composites and stabilised by interlocking polymer rivets. The rivets' structure improves the load-bearing performance of the composites without any modification to the battery itself [265]. Thin-film supercapacitors can also be used in the replacement of thin-film batteries. Senokos et al. [266] fabricated multi-layered structural energy storage composites by embedding thin sandwich structure supercapacitors as an interleaf between carbon fibre plies.

However, these approaches somewhat fly in the face of the concept of energy-storing composites. The idea is to take a structural component of a spacecraft and make this component intrinsically energy-storing—this way, the weight of the spacecraft can be reduced owing to the reduction in the battery pack. Embedding a low-profile battery into structural composites does not eliminate the weight of the battery pack; it distributes it. Recently, however, an attractive alternative approach to realising energy-storing composites has been realised, fabricating composites that intrinsically form an energy storage device. This involves using carbon fibre as electrodes, a thin-film porous polymer or fibre glass separator, a conductive polymer electrolyte and a resin (typically epoxy-based). As illustrated in Fig. 14, a laminated structure is the most common configuration for structural supercapacitor composites. Two carbon fibre mats used as electrodes with glass fabrics as separators in the middle, followed by infusing of multifunctional polymer electrolyte, were first introduced by Shirshova et al. [267]. Today, much research is aspiring to develop effective intrinsically energy-storing structural composites. Paving the way in this field are the developers of SORCERER (Structural pOweR CompositEs foR futurE civil aiRcraft) technology. This research is being

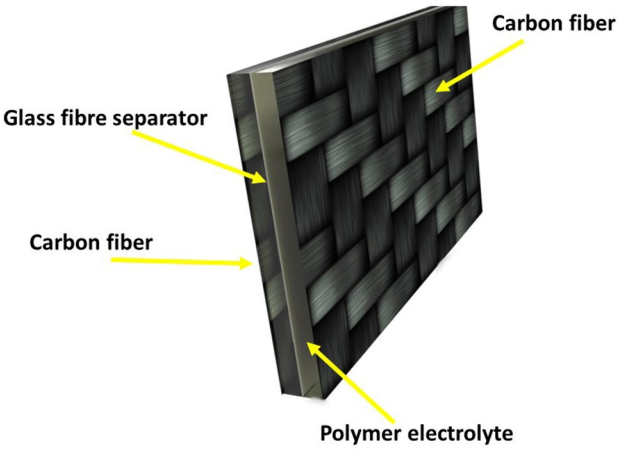

Fig. 14 Schematic configuration of structural supercapacitor composites [240]

completed collaboratively through the Imperial College of London, Chalmers University of Technology, KTH Royal Institute of Technology (Sweden) and IMDEA Networks Institute. Together, the researchers have been developing structurally robust carbon fibre and graphitic electrodes to serve as the next-generation energy storage composite electrodes and simultaneously develop high mechanical strength and highly conductive electrolyte resins [268]. Also, very recently, a graphene aerogel–modified carbon fibre energy-storing composite was reported in the literature [269]. Subhani and others [269] employed graphene aerogel–coated carbon fibre as the electrodes, an ultra-thin electrospun nanofibre separator and an ionic liquid epoxy electrolyte. A high capacitance of 92.5 F g^{-1} at 1 mV s^{-1} was achieved, as well as capacitance retention of 98% after 10,000 charge cycles.

However, energy storage composites' density, volume and weight are generally increased when attempting to fabricate energy storage composites. In addition, the mechanical properties are often considerably compromised. Specifically, new electrolyte candidates are urgently needed. A structural energy-storing composite ideally has good ion transport and high mechanical load-bearing. These two properties can be challenging to achieve in an electrolyte since they are often contradictory [270]. A compromise between mechanical performance and ionic conductivity is sometimes unavoidable to achieve optimum multifunctional enhancement, as they are inversely related. There is, however, still promise for incorporating nanotechnologies, such as graphene and other enhancement fillers with superior mechanical properties, into the resins of energy storage composites, as a way of improving the mechanical strength lost in the process of making the composites energy-storing.

8.2 Structural health-monitoring composites

Structural health monitoring (SHM) is an emerging means of detecting structural failure or degradation in real time. SHM smart composites involve fabricating structural components with the additional functionality of health-monitoring detection. This imparts the composite and health-monitoring technology with a symbiotic-like relationship—structurally robust composites protect the health-monitoring components, and the health-monitoring components help keep the composites structurally strong. This also results in a reduction in weight and fuel consumption, stemming from integrating what were once two separate parts into one, ultimately improving feasibility. It also transforms the traditional regimens of condition monitoring techniques into the evolution of a *smarter* system with self-sensing capability. The system safety and stability can thus be improved by timely evaluation of structural integrity.

Polymeric composites are ideal candidates for designing self-diagnosing SHM smart composites. Piezoresistance is the most commonly explored mechanism for achieving SHM based on real-time in situ strain response. Four common fabrication techniques are adopted to realise piezoresistant SHM composites: self-sensing CFRPC; impregnation with piezoresistive matrices; integration of conductive filaments, additives and yarns during fabrication procedure; and surface integration with piezoresistive films, as shown in Table 4. Yao et al. [271] demonstrated the conductivity of carbon fibre can be used to realise CFRP smart self-sensing composites. The occurrence of damage alters the conductivity of the carbon fibre, which can be measured, enabling detection. The printed composites are capable of SHM functionality with improved tensile strength (70%) and flexural strength (18.7%). However, such an approach is only suitable for composites with conductive fibres like carbon fibre, and the matrix-dominated failure mode is undetectable. Nasir et al. [272] also reported carbon nanoparticle/polystyrene glass fibre epoxy composites can also act as effective self-sensing structural health-monitoring composites. De Simone et al. [273] reported the same with thin-film PZT-integrated carbon fibre composites. When high-velocity impacts occurred, the PZT film could detect the damage and accurately locate the impact site. CNT twisted threads could also be embedded in composites for SHM, as reported by Wan et al. [274]. The tested specimen could provide linear testing results for loading up to 650 MPa.

Both self-sensing carbon fibre–reinforced composite (CFRC) and piezoresistive matrix techniques have limitations as they can only detect one type of failure (either matrix dominated or fibre dominated) due to their inherent nature. Surface-mounted sensor techniques can only provide real-time strain information but are not able to show any detailed information about damage type, initiation or propagation. Among all the adopted technologies, the embedment of filaments is an ideal technique, as it is inserted inside composites during the fabrication process; it can provide valuable information for SHM and detect all types of composites' failure during service.

8.3 EMI shielding in composites

Another functionality capable of being endowed into structural composites is EMI shielding. As previously discussed, EMI shielding is a crucial capability for spacecraft. Also previously discussed is the nature of EMI shielding materials to come in the form of coatings or thin films. With EMI shielding composites, the entire component also doubles as an EMI shield, negating the necessity for additional EMI shielding coatings. This may seem impractical to resort to fabricating a large multifunctional component when the issue can be overcome with a simple thin film or coating application. However, a lot of the materials already used in composites are conductive and electron-dense, making them intrinsically EMI shielding. CFRC has been widely used as EMI shielding materials with an EMI SE of 115 dB over the frequency range from 0.3 MHz to 1.5 GHz [275]. With the advanced development of nanotechnology, there is also the potential to incorporate conductive fillers such as CNTs and graphene into CFRP resins, improving the thermal and electrical conductivity and, therefore, EMI shielding capability. Recently, Yan et al. [276] reported an impressive high-performance EMI shielding smart composite material [249]. The authors combined reduced graphene oxide and polystyrene. The authors reported that the reduced graphene

Table 4 Comparison of four common SHM techniques

Sensing mechanism	Sensitivity	Sensing capability	Disadvantage
Self-sensing composites (CFRC)	Non-modifiable	Fibre-dominated failure	Matrix-dominated failure not detectable
Piezoresistive matrix	Modifiable within a certain range	Matrix-dominated failure	Fibre-dominated failure not detectable
Surface-integrated sensors	Modifiable	Strain sensing	Strain response is not correlated with various failure types
Embedded filaments/yarns	Modifiable	Fibre/matrix failure	–

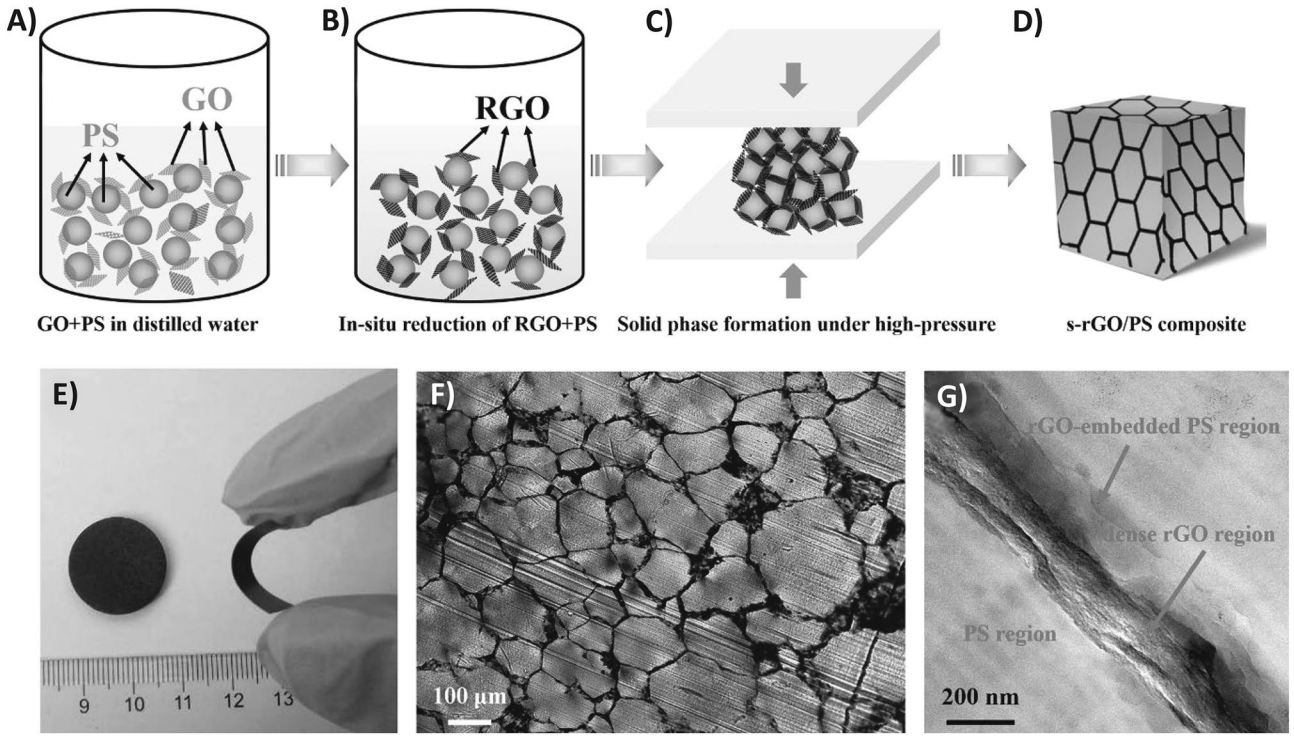

Fig. 15 Depiction of PS-GO EMI shielding composite material. **A**) demonstrating the functionalization of PS with GO; **B**) Illustrating the in-situ reduction of GO/PS mixture; **C**) Illustrating the high-pressure formation of solid phase rGO/PS composite material; **D**) Illustrating the resultant rGO/PS composite material; **E**) optical photograph of composite material thin film demonstrating material flexibility; **F**) crosssection optical microscopy image of rGO/PS composite material; **G**) TEM image of rGO layers between PS regions. Reproduced with permission [276]. Copyright year, Publisher.

oxide forms a highly conductive coating on the composite surface, which is highly effective for multiple reflection and scattering (see Fig. 15). The material showed good mechanical properties, good processability and excellent EMI SE value (up to 45.1 dB at 8.2 GHz) with a rGO loading of 3.47% [276]. This research holds potential for the production of robust and cheap EMI shielding components that are not required to bear large mechanical loads.

The main hurdle with smart composite technologies is overcoming the trade-off between mechanical strength and functional performance. Both energy storage and SHM composites exhibit sub-par mechanical properties to pristine CFRPCs. The exception is EMI shielding composites. The addition of nanofillers such as CNTs or graphene into CFRPC resin matrices generally improves EMI SE, electrical and thermal conductivity and mechanical strength and reduces the weight. For now, the current approaches to EMI shielding for space lie outside of the realm of smart composite technology, largely due to the progress made in processability and ease of fabrication in EMI thin films and coatings. However, the trend in technological development is to make technology more compact, functional and integrated. Inevitably, this leads to the demand for smart composites, including EMI shielding. This technology is still relatively novel and ahead of its time. There are many problems to be overcome and many questions to be answered. Yet, it cannot be denied that the structural components of a spacecraft, infamously, significantly contribute to the spacecraft's weight. It is only logical to attempt to correct this inefficiency.

9 Conclusion

The reported materials' applications are related to improving safety, functionality or feasibility for spacecraft and space-bound technologies. Additional capabilities can be developed by mitigating the threats or addressing the challenges experienced during space travel. Challenges encompass damage from micro-meteorites/space debris or UV radiation, the dangers of fire in space, extremes of temperature, space dust and its adverse risks, effects of EMI on communications and navigation and the associated cost of transporting heavy machinery and technologies out of Earth's orbit. This review articulates and summarises the latest progress and development in emerging materials with applications in space. The materials focused on this review hold great potential and warrant the tremendous efforts currently being made to further the efficiency, functionality or ease of materials fabrication. Progressive research and development into

the materials outlined in this review will better equip spacecraft, crew and future inter-planetary colonies for dealing with and navigating the hostile unforgiving environments experienced during space travel.

9.1 Future outlooks

We began this review by discussing the challenges and risks associated with space travel and how materials can potentially solve or mitigate said difficulties and dangers. Materials for space applications often centre around crew safety, spacecraft longevity and mission feasibility—future materials for space must be adaptive, multifunctional and self-healing. Throughout this review, we discussed the next generation of emerging materials for space applications that address these motifs. Self-healing polymers naturally hold great potential for space applications. However, overcoming the limitations of one-time-only self-healing in intrinsic self-healing materials is still a significant challenge. Without doing so, the applicability of self-healing materials in space becomes considerably reduced. Ultimately, this demands the development of novel materials, which is no trivial task. Extrinsic self-healing materials are capable of repeatable self-healing; however, the necessity for an input of energy to initiate the self-healing process in these materials poses a challenge when in space. Polymeric nanofiller (carbides, titania nanomaterials, graphene, its derivatives and MXenes) hybrid films show great potential in several applications, from EMI shielding or thermal management to self-cleaning surfaces or fire-resistant materials. Fine-tuning, optimising and understanding the processing of advanced materials through proper handshaking between level-specific modelling techniques will expectedly improve the performance and feasibility of these materials.

The areas ripe for innovation, outlined in the paragraph above, are technical challenges that must be overcome through iterative and explorative improvements; they are essential in their own right. Yet, it is also possible to forecast the grander approaching outlooks for space materials. The ultimate goal would be integrating multiple functionalities into a single component/material. For example, combining self-healing technology with structural health-monitoring composites can potentially improve the safety, longevity and feasibility of materials for space applications, simultaneously. Similarly, a spacecraft with intrinsically EMI shielding/energy-storing composite structural panels would spell both a reduction in weight and profile, improving feasibility. Combining self-healing materials with self-cleaning surfaces could enable scratch and dust-resistant coatings, improving solar panel longevity and feasibility.

Integrating numerous functionalities into a single material often brings inherent challenges in maintaining the original functionalities. Energy-storing structural components, for example, often suffer from losses in mechanical properties compared to new structural features. Continuous progress in quantum computing/artificial intelligence will yield such or similar materials/technologies through advanced materials modelling. It may 1 day be possible to have a satellite that uses its structural panels as antennas and power sources, can shape morph, is self-healing, has adequate EMI shielding capabilities, is self-cleaning and is thermally stable. Till then, there is considerable research to be done in the area of space materials.

Author contribution M. P. and J. I.: formal analysis, writing the initial draft and review and editing; L. M., A. P., A. A., S. A. and Y. Y.: writing the initial draft and review and editing; N. H., A. D. and A. L.: writing and review and editing; N. S.: supervision, project administration, conceptualization and design, writing the initial draft and review and editing.

Funding Open Access funding enabled and organized by CAUL and its Member Institutions.

Declarations

Competing interests The authors declare no competing interests.

References

1. UCS Satellite Database. Union of Concerned Scientists. https://www.ucsusa.org/resources/satellite-database. Accessed 15 May 15 2023
2. Zavada SR, McHardy NR, Gordon KL, Scott TF (2015) ACS Macro Lett 4:819
3. Zamal HH, Barba D, Aïssa B, Haddad E, Rosei F (2021) Smart Mater Struct 30
4. Gradl PR, Valentine PG (2017) In 53rd AIAA/SAE/ASEE Joint Propulsion Conference, 2017. American Institute of Aeronautics and Astronautics Inc., AIAA
5. Brian D (2019) Woven Mater
6. Cai H, Jiang Y, Feng J, Chen Q, Zhang S, Li L, Feng J (2020) Ceram Int 46:12489
7. Belobrajdic B, Melone K, Diaz-Artiles A (2021) NPJ Microgravity 7:1
8. Manyapu KK, Peltz L, de Leon P (2019) Acta Astronaut 157:134
9. Calle CI, Mackey PJ, Hogue MD, Johansen MR, Yim H, Delaune PB, Clements JS (2013) J Electrostat 71:257
10. Roslizar A, Dottermusch S, Schmager R, Guttmann M, Gomard G, Hölscher H, Richards BS, Paetzold UW (2020) Sol Energy Mater Sol Cells 214:110582

11. Kamsali N, Chakravarty SC, Basuvaraj PK (2019) Heliyon 5:e02972
12. Nambiar S, Yeow JTW (2012) ACS Appl Mater Interfaces 4:5717
13. Ma L, Lu Z, Tan J, Liu J, Ding X, Black N, Li T, Gallop J, Hao L (2017) ACS Appl Mater Interfaces 9:34221
14. Naguib M, Kurtoglu M, Presser V, Lu J, Niu J, Heon M, Hultman L, Gogotsi Y, Barsoum MW (2011) Adv Mater 23:4248
15. Lopez CF, Jeevarajan JA, Mukherjee PP (2016) J Electrochem Energy Conversion Storage 13
16. Ortona A, Pusterla S, Gianella S (1821) J Eur Ceram Soc 2011:31
17. Fredi G, Jeschke S, Boulaoued A, Wallenstein J, Rashidi M, Liu F, Harnden R, Zenkert D, Hagberg J, Lindbergh G, Johansson P, Stievano L, Asp LE (2018) Multifunct Mater 1:15003
18. Levchenko I, Bazaka K, Belmonte T, Keidar M, Xu S (2018) Adv Mater 30:1802201
19. Levchenko I, Xu S, Mazouffre S, Keidar M, Bazaka K (2019) Global Chall 3:1800062
20. Camargo PHC, Satyanarayana KG, Wypych F (2009) Mater Res 12:1
21. Peraza-Hernandez EA, Hartl DJ, Malak Jr RJ, Lagoudas DC (2014) Smart Mater Struct 23:094001
22. Huang Y, Zhu M, Huang Y, Pei Z, Li H, Wang Z, Xue Q, Zhi C (2016) Adv Mater 28:8344
23. Alpert BK, Johnson BJ (2019) In 49th International Conference on Environmental Systems. Boston, Massachusetts, p 30
24. Degtyarev AV, Lobanov LM, Kushnar'ov AP, Baranov IY, Volkov VS, Perepichay AO, Korotenko VV, Volkova OA, Osinovyy GG, Lysenko YA, Kaliapin MD (2020) Acta Astronaut 170:487
25. Naser MZ, Chehab AI (2018) Materials and design concepts for space-resilient structures, Vol 98, Elsevier Ltd, pp 74–90
26. Buslov EP, Komarov IS, Selivanov VV, Titov VA, Tovarnova NA, Feldstein VA (2019) Acta Astronaut 163:54
27. Cadogan D, Scheir C, Dixit A, Ware J, Cooper E, Kopf P (2006) In Collection of technical papers - AIAA/ASME/ASCE/AHS/ASC Structures, Structural Dynamics and Materials Conference, pp 3705–3721
28. Ekeocha J, Ellingford C, Pan M, Wemyss AM, Bowen C (2021) C Wan 2008052:1
29. Guo W, Jia Y, Tian K, Xu Z, Jiao J, Li R, Wu Y, Cao L, Wang H (2016) ACS Appl Mater Interfaces 8:21046
30. Mishra S, Chaudhary P, Yadav BC, Umar A, Lohia P, Dwivedi DK (2021) Eng Sci 15:138
31. Chen D, Wang D, Yang Y, Huang Q, Zhu S, Zheng Z
32. Li P, Guo W, Lu Z, Tian J, Li X, Wang H (2021) Prog Org Coat 151:106046
33. Li P, Lu Z, Ma K, Zou G, Chang L, Guo W, Tian K, Li X, Wang H (2022) Prog Org Coat 163:106636
34. Zhu Y, Cao K, Chen M, Wu L (2019) ACS Appl Mater Interfaces 11:33314
35. Gao L, Yang Y, Xie J, Zhang S, Hu J, Zeng R, He J, Li Q, Wang Q (2020) Matter 2:451
36. White SR, Moore JS, Sottos NR, Krull BP, Santa Cruz WA, Gergely RCR (2014) Science (1979) 344:620
37. Lei XF, Chen Y, Zhang HP, Li XJ, Yao P, Zhang QY (2013) ACS Appl Mater Interfaces 5:10207
38. Jolley ST, Williams MK, Gibson TL, Smith TM, Caraccio AJ, Li W (2012) Self-healing polymer materials for wire insulation, polyimides, flat surfaces, and inflatable structures, US Patent Office, USA
39. Wang X, Li Y, Qian Y, Qi H, Li J, Sun J (2018) Adv Mater 30:1
40. Song T, Jiang B, Li Y, Ji Z, Zhou H, Jiang D, Seok I, Murugadoss V, Wen N, Colorado H (2021) ES Mater Manuf 14:1
41. Liu J, Zheng N, Li Z, Liu Z, Wang G, Gui L, Lin J (1899) Adv Compos Hybrid Mater 2022:5
42. Aissa B, Haddad E, Jamroz W, Hassani S, Farahani RD, Merle PG, Therriault D (2012) Smart Mater Struct 21:8
43. Feng X, Li G (2021) ACS Appl Mater Interfaces 13:53099
44. Putnam-Neeb AA, Kaiser JM, Hubbard AM, Street DP, Dickerson MB, Nepal D, Baldwin LA (2022) Adv Compos Hybrid Mater 5:3068
45. Chen F, Xiao H, Peng ZQ, Zhang ZP, Rong MZ, Zhang MQ (2021) Adv Compos Hybrid Mater 4:1048
46. Liu C, Yin Q, Li X, Hao L, Zhang W, Bao Y, Ma J (2021) Adv Compos Hybrid Mater 4:138
47. Madara SR, Raj Sarath NS, Selvan CP (2018) IOP Conf Ser Mater Sci Eng 346
48. Sun D, Yan J, Ma X, Lan M, Wang Z, Cui S, Yang J (2021) ES Mater Manuf 14:59
49. Zhao Y, Liu K, Zhang H, Tian X, Jiang Q, Murugadoss V, Hou H (2022) Adv Compos Hybrid Mater 5:2546
50. Fisher Jr CRJJM , Henderson HB, Kesler MS (2019) Manuel MV Front Mater 6:1
51. Fisher CR, Henderson HB, Kesler MS, Zhu P, Bean GE, Wright MC, Newman JA, Brinson LC, Figueroa O, Manuel MV (2018) Appl Mater Today 13:64
52. Nambiar SS, Murthy BRN, Sharma S, Prasanna AA, Chelvane AJ (2022) Eng Sci17:303
53. Song M, Wang J, Yuan L, Luan C, Zhou Z (2022) ES Mater Manuf 17:23
54. Wu P, Wang Z, Yao X, Fu J, He Y (2006) Mater Horiz 2021:8
55. Wang J, Yuan Y, Li C, Su W, Abo-Dief HM, Zhang C, Huang M, Abualnajad KM, Alanazid AK, Zhu XF, Seok I (2022) Adv Compos Hybrid Mater 5:1450
56. Danzi S, Schnabel V, Gabl J, Sologubenko A, Galinski H, Spolenak R (2019) Adv Mater Technol 4:1
57. Nakao W, Abe S (2012) Smart Mater Struct 21
58. Tong Y, Wang L, Wang B, Hu Y, Cai Z, Ren J, Liu J, Li S (2023) Adv Compos Hybrid Mater 6:1
59. Shao G, Lu Y, Hanaor DAH, Cui S, Jiao J, Shen X (2019) Corros Sci 146:233
60. Kauffman J (1999) Public Relat Rev 25:421
61. Buckley JD, Edie DD (1999) Carbon-carbon materials and composites - 1st Edition, 1st ed., Elsevier
62. Burchell TD (1999) Carbon materials for advanced technologies. Elsevier
63. Knapschaefer J (2016) NASA/Boeing composite launch vehicle fuel tank scores firsts | CompositesWorld
64. Karthik A, Chiniwar DS, Das M, Pai PM, Prabhu P, Mulimani PA, Samanth K, Naik N (2021). 16:129. https://www.espublisher.com/
65. NASA, Silicon carbide (SiC) fiber-reinforced SiC matrix composites
66. Turner JE (2017) In The quest for engineering innovation at NASA's Marshall Space Flight (MSFC). Colorado State University, Professional Learning Institute, NASA
67. Jacobs SE, Tufts DB, Gohmert DM (2018) In 48th International Conference on Environmental Systems, Albuquerque, New Mexico
68. Ozdemir E, Arenas DR, Kelly NL, Hanna JV, van Rijswijk B, Degirmenci V, McNally T (2020) Polymer (Guildf) 205:122836
69. Hebalkar N, Kollipara KS, Ananthan Y, Sudha MK (2020) In Handbook of advanced ceramics and composites. Springer International Publishing, pp 121–163
70. Peng F, Jiang Y, Feng J, Cai H, Feng J, Li L (2021) Chem Eng J 411:128402
71. Dou L, Cheng X, Zhang X, Si Y, Yu J, Ding B (2020) J Mater Chem A Mater 8:7775
72. Johnson SM (2012) Thermal protection materials: development, characterization and evaluation

73. Courtright EL, Graham HC, Katz AP, Kerans RJ (1992) Ultra-high temperature assessment study: ceramic matrix composites
74. Yasnó JP, Gunnewiek RFK, Kiminami RHGA (2019) Adv Powder Technol 30:1348
75. Albano M, Morles RB, Cioeta F, Marchetti M (2014) Acta Astronaut 99:276
76. Heidman K (2015) Advancing ceramic coatings for engine life and efficiency
77. Bauer PE, Kummer DL (1966) J Spacecr Rockets 3:1495
78. Johanna J (2016) NASA/Boeing composite launch vehicle fuel tank scores firsts | CompositesWorld
79. Dombrowski RD, Wagner NJ, Katzarova M, Peters BJ (2018) 48th International Conference on Environmental Systems
80. Bristol P (2014) Multi-layer insulation films and tapes from DUNMORE Protect ESA's Rosetta Mission for Over 10 Years in Space
81. Stem Cell, Beta Cloth Swatch
82. NASA. About the sunshield
83. Darling S (2018) Travelling to the sun: why won't Parker Solar Probe melt
84. Guerges M (2021) Tests landing pad materials for future lunar missions
85. Campbell AI, Martin LE, Murai VRT, Ramirez FS, Carson HC, de Soto M, English KA, Fiske MR, Romo EM, Schang KE, Smith KC, Scitech AIAA (2021) Forum 2021:1
86. Company A, America OF, Aeronautics N
87. Weiss P, Mohamed MP, Gobert T, Chouard Y, Singh N, Chalal T, Schmied S, Schweins M, Stegmaier T, Gresser GT, Groemer G, Sejkora N, Das S, Rampini R (2020) M Hołyńska 2000028:1
88. Fesmire JE, Johnson WL (2018) Cryogenics (Guildf) 89:58
89. Milos FS, Squire TH (1995) In Thermal stress analysis of RCG-tempered TUFI tile TPS for hypersonic vehicles, NASA
90. White S, Rasky D, Herlth P (2016). 7857
91. Johnson SM (2016)
92. Yu SY, Ganev EG (2009) SAE Int J Aerosp 1:1107
93. Hyun C, Park S (1992) Analysis of thermally induced damage in composite space structures. U Professor Harold Y Wachman. Massachusetts Institute of Technology
94. Esser B, Barcena J, Kuhn M, Okan A, Haynes L, Gianella S, Ortona A, Liedtke V, Francesconi D, Tanno H (2016) J Spacecr Rockets 53:1051
95. Ochoa HA, Hua J, Lee R, Mastropietro AJ, Bhandari P, Paris A, Lok D, Emis N, Bertagne C (2017)
96. Stephan RA (2010) In 40th Int Conf Environ Syst
97. Plough AH, Pavarani AA (1999) In SAE Technical Papers, SAE International
98. EPM IR Thermal Imager
99. Dai W, Lv L, Lu J, Hou H, Yan Q, Alam FE, Li Y, Zeng X, Yu J, Wei Q, Xu X, Wu J, Jiang N, Du S, Sun R, Xu J, Wong CP, te Lin C (2019) ACS Nano 13:1547
100. Song H, Liu J, Liu B, Wu J, Cheng HM, Kang F (2018) Joule 2:442
101. Sarvar F, Whalley DC, Conway PP (2006) In ESTC 2006 - 1st Electronics System-Integration Technology Conference. Institute of Electrical and Electronics Engineers Inc pp 1292–1302
102. Barani Z, Mohammadzadeh A, Geremew A, Huang CY, Coleman D, Mangolini L, Kargar F, Balandin AA (2020) Adv Funct Mater 30:1904008
103. Uetani K, Ata S, Tomonoh S, Yamada T, Yumura M, Hata K (2014) Adv Mater 26:5857
104. Zhou Y, Zhuang X, Wu F, Liu F (2018) Crystals (Basel) 8:398
105. Varadan VK, Vinoy KJ, Gopalakrishnan S (2006) Smart material systems and MEMS: design and development methodologies | Wiley, John Wiley & Sons
106. Shtein M, Nadiv R, Buzaglo M, Regev O (2015) ACS Appl Mater Interfaces 7:23725
107. Yu W, Xie H, Chen L, Wang M, Wang W (2017) Polym Compos 38:2221
108. Yu L, Park JS, Lim YS, Lee CS, Shin K, Moon HJ, Yang CM, Lee YS, Han JH (2013) Nanotechnology 24
109. Cui X, Ding P, Zhuang N, Shi L, Song N, Tang S (2015) ACS Appl Mater Interfaces 7:19068
110. Yu J, Choi HK, Kim HS, Kim SY (2016) Compos Part A Appl Sci Manuf 88:79
111. Sun R, Yao H, Zhang HB, Li Y, Mai YW, Yu ZZ (2016) Compos Sci Technol 137:16
112. Liu C, Chen C, Wang H, Chen M, Zhou D, Xu Z, Yu W (2019) Polym Compos 40:E1294
113. Shao L, Shi L, Li X, Song N, Ding P (2016) Compos Sci Technol 135:83
114. Zhao B, Wang S, Zhao C, Li R, Hamidinejad SM, Kazemi Y, Park CB (2018) Carbon N Y 127:469
115. Du FP, Yang W, Zhang F, Tang CY, Liu SP, Yin L, Law WC (2015) ACS Appl Mater Interfaces 7:14397
116. Yang SY, Lin WN, Huang YL, Tien HW, Wang JY, Ma CCM, Li SM, Wang YS (2011) Carbon N Y 49:793
117. Im H, Kim J (2012) Carbon N Y 50:5429
118. Gallego NC, Klett JW (2003) Carbon N Y 41:1461
119. Reimer T, Petkov I, Rotärmel W (2015) 8th European Symposium on Aerothermodynamics for Space Vehicles
120. Fan W, Zhang G, Zhang X, Dong K, Liang X, Chen W, Yu L, Zhang Y (2022) Small 18:2270049
121. Kim K, Ju H, Kim J (2016) Compos Sci Technol 123:99
122. Pak SY, Kim HM, Kim SY, Youn JR (2012) Carbon N Y 50:4830
123. Lee S, Yang F, Suh J, Yang S, Lee Y, Li G, Choe HS, Suslu A, Chen Y, Ko C, Park J, Liu K, Li J, Hippalgaonkar K, Urban JJ, Tongay S, Wu J (2015) Nat Commun 6:1
124. Ling Z, Chen J, Fang X, Zhang Z, Xu T, Gao X, Wang S (2014) Appl Energy 121:104
125. Ling Z, Zhang Z, Shi G, Fang X, Wang L, Gao X, Fang Y, Xu T, Wang S, Liu X (2014) Renew Sustain Energy Rev 31:427
126. Patel NV (2020) Current spacesuits won't cut it on the moon. So NASA made new ones. | MIT Technology Review
127. Harvey GA, Humes DH, Kinard WH (2000) High Perform Polym 12:65
128. (2020) Solar panel obscuration by dust and dust mitigation in the Martian atmosphere. Particles on Surfaces: Detection, Adhesion and Removal, Vol 9, CRC Press, pp 175–204
129. Calle CI, Buhler CR, Johansen MR, Hogue MD, Snyder SJ (2011) Acta Astronaut 69:1082
130. Blossey R (2003) Nat Mater 2:301
131. Pirich R, Weir J, Leyble D (2008) In Optical system contamination: effects, measurements, and control 2008, SPIE, p 70690B
132. Jenner L (2019)
133. Granath B (2015)
134. Patankar NA (2004) Langmuir 20:8209
135. Bhushan B, Jung YC (2011) Natural and biomimetic artificial surfaces for superhydrophobicity, self-cleaning, low adhesion, and drag reduction, Vol 56, Elsevier Ltd, pp 1–108
136. Margiotta DV, Peters WC, Straka SA, Rodriguez M, McKittrick KR, Jones CB (2010) In Optical system contamination: effects, measurements, and control 2010, SPIE, p 77940I
137. Dove A, Devaud G, Wang X, Crowder M, Lawitzke A, Haley C (2011) In Planetary and space science, Pergamon, pp 1784–1790
138. Law KY, Zhao H (2015) Surface wetting: characterization, contact angle, and fundamentals, Springer International Publishing
139. Shirtcliffe NJ, McHale G, Atherton S, Newton MI (2010) An introduction to superhydrophobicity, Vol 161, Elsevier, pp 124–13861
140. Pirich RG (2009) J Nanophotonics 3:031870
141. Roslizar A, Dottermusch S, Vüllers F, Kavalenka MN, Guttmann M, Schneider M, Paetzold UW, Hölscher H, Richards BS, Klampaftis E (2019) Sol Energy Mater Sol Cells 189:188

142. Devaud G, Haley C, Rockwell C, Fischer A (2014) In Systems contamination: prediction, measurement, and control 2014, SPIE, p 919603
143. Chen S, Li X, Li Y, Sun J (2015) ACS Nano 9:4070
144. Cao C, Ge M, Huang J, Li S, Deng S, Zhang S, Chen Z, Zhang K, Al-Deyab SS, Lai Y (2016) J Mater Chem A Mater 4:12179
145. Zhu S, Kang Z, Wang F, Long Y (2021) Nanotechnology 32:035701
146. Shateri-Khalilabad M, Yazdanshenas ME (2013) Cellulose 20:963
147. Karimi L, Yazdanshenas ME, Khajavi R, Rashidi A, Mirjalili M (2014) Cellulose 21:3813
148. Stan MS, Nica IC, Popa M, Chifiriuc MC, Iordache O, Dumitrescu I, Diamandescu L, Dinischiotu A (2019) J Ind Text 49:277
149. Adams J, Cline B, Contaxes N, Johnson RD, Seaman H, Srepel V, Tatom F (1967) Lunar dust degradation effects and removal/prevention concepts. Volume 1 - Summary Final Report
150. Afshar-Mohajer N, Wu CY, Curtis JS, Gaier JR (2015) Adv Space Res 56:1222
151. Fernandez D, Cabas R, Moreno L (2007) In Industrial and commercial applications of smart structures technologies 2007, SPIE, p 65270E
152. Bernard AR, Eriksen R, Horenstein MN, Mazumder MK (2018) MRS Energy Sustain 5:1
153. Jones D, Bernard AR, Hoffman M, Chang S, Wilkins C, Eriksen R, Ellinger C, Garner S, Rothacker A, Thellen C, Mazumder M (2020) MRS Adv 5:2595
154. Masuda S, Kamimura T (1975) J Electrostat 1:351
155. Biris AS, Saini D, Srirama PK, Mazumder MK, Sims RA, Calle CI, Buhler CR (2004) In Conference Record - IAS Annual Meeting (IEEE Industry Applications Society) pp 1283–1286
156. Mazumder MK, Sharma R, Biris AS, Zhang J, Calle C, Zahn M (2007) Part Sci Technol 25:5
157. Sharma R, Wyatt CA, Zhang J, Calle CI, Mardesich N, Mazumder MK (2009) IEEE Trans Ind Appl 45:591
158. Calle CI, Arens EE, McFall JM, Buhler CR, Snyder SJ, Geiger JK, Hafley RA, Taminger KM, Mercer CD (2009) In IEEE Aerospace Conference Proceedings
159. Kawamoto H, Hara N (2011) J Aerosp Eng 24:442
160. Kawamoto H (2014) J Aerosp Eng 27:354
161. Jiang J, Lu Y, Yan X, Wang L (2020) Acta Astronaut 166:59
162. Turer I, Aydin KAUGA (2015) Ears ITAFAITUBUMETUY TURHTATAITEIIPALPHMES. IEEE, TSSHMSI. Defence Technologies SSDSEMIEMC Turkish Aerosp Ind Inc Tai AT. Rf Design Grp, In 7th International Conference on Recent Advances in Space Technologies (RAST), IEEE, Istanbul, Turkey, pp 401–404
163. Modus Team (2021) 5 considerations for EMI shielding in space applications
164. Yao F, Xie W, Ma C, Wang D, El-Bahy ZM, Helal MH, Liu H, Du A, Guo Z, Gu H (2022) Compos B Eng 245:110236
165. Shivamurthy RBJCRB, Gowda SBB, Kumar MS (2022). 21:777. https://www.espublisher.com/
166. Pai AR, Binumol T, Gopakumar DA, Pasquini D, Seantier B, Kalarikkal N, Thomas S (2020) Carbohydr Polym 246:116663
167. Gopakumar DA, Pai AR, Pottathara YB, Pasquini D, Carlos De Morais L, Luke M, Kalarikkal N, Grohens Y, Thomas S (2018) ACS Appl Mater Interfaces 10:20032
168. Gopakumar DA, Pai AR, Pottathara YB, Pasquini D, de Morais LC, Khalil AHPS, Nzihou A, Thomas S (2021) J Appl Polym Sci 138:50262
169. Pai AR, Paoloni C, Thomas S (2021) In Nanocellulose based composites for electronics, Elsevier, pp 237–258
170. Gupta S, Tai NH (2019) Carbon N Y 152:159
171. Abbasi H, Antunes M, Velasco JI (2019) Prog Mater Sci 103:319
172. Wang M, Tang XH, Cai JH, Wu H, Shen JB, Guo SY (2021) Carbon N Y 177:377
173. Kong L, Yin XW, Xu HL, Yuan XY, Wang T, Xu ZW, Huang JF, Yang R, Fan H (2019) Carbon N Y 145:61
174. Liang CB, Qiu H, Han YY, Gu HB, Song P, Wang L, Kong J, Cao DP, Gu JW (2019) J Mater Chem C Mater 7:2725
175. Hu PY, Lyu J, Fu C, Gong WB, Liao JH, Lu WB, Chen YP, Zhang XT (2020) ACS Nano 14:688
176. Song P, Liu B, Liang CB, Ruan KP, Qiu H, Ma ZL, Guo YQ, Gu JW (2021) Nanomicro Lett 13:17
177. Wang L, Shi XT, Zhang JL, Zhang YL, Gu JW (2020) J Mater Sci Technol 52:119
178. Guo Y, Liu H, Wang D, El-Bahy ZM, Althakafy JT, Abo-Dief HM, Guo Z, Xu BB, Liu C, Shen C (2022) Nano Res 15:6841
179. Wei QW, Pei SF, Qian XT, Liu HP, Liu ZB, Zhang WM, Zhou TY, Zhang ZC, Zhang XF, Cheng HM, Ren WC (2020) Adv Mater 32:9
180. Lai D, Chen X, Wang G, Xu X, Wang Y (2020) J Mater Chem C Mater 8:8904
181. Cheng H, Lu Z, Gao Q, Zuo Y, Liu X, Guo Z, Liu C, Shen C (2021) Eng Sci 16:331
182. Luan WY, Wang Q, Sun Q, Lu YX (2021) Chin J Aeronaut 34:91
183. Wang L, Qiu H, Liang CB, Song P, Han YX, Han YX, Gu JW, Kong J, Pan D, Guo ZH (2019) Carbon N Y 141:506
184. Huangfu YM, Liang CB, Han YX, Qiu H, Song P, Wang L, Kong J, Gu JW (2019) Compos Sci Technol 169:70
185. Shen B, Zhai W, Zheng W (2014) Adv Funct Mater 24:4542
186. Lee HD, Yoo BM, Lee TH, Park HB (2018) J Colloid Interface Sci 509:307
187. Tung VC, Chen LM, Allen MJ, Wassei JK, Nelson K, Kaner RB, Yang Y (1949) Nano Lett 2009:9
188. Li Y, Pei X, Shen B, Zhai W, Zhang L, Zheng W (2015) RSC Adv 5:24342
189. Wang YY, Zhou ZH, Zhou CG, Sun WJ, Gao JF, Dai K, Yan DX, Li ZM (2020) ACS Appl Mater Interfaces 12:8704
190. Inagaki M, Ohta N, Hishiyama Y (2013) Aromatic polyimides as carbon precursors, Vol 61, Pergamon, pp 1–21
191. Liu H, Wu S, Tian N, Yan F, You C, Yang Y (2020) Carbon foams: 3D porous carbon materials holding immense potential, Vol 8, Royal Society of Chemistry, pp 23699–23723
192. Li Y, Shen B, Pei X, Zhang Y, Yi D, Zhai W, Zhang L, Wei X, Zheng W (2016) Carbon N Y 100:375
193. Duong-Viet C, Ba H, El-Berrichi Z, Nhut JM, Ledoux MJ, Liu Y, Pham-Huu C (2016) New J Chem 40:4285
194. Hotza D, Di Luccio M, Wilhelm M, Iwamoto Y, Bernard S, Diniz da Costa JC (2020) J Memb Sci 610:118193
195. Eom JH, Kim YW, Raju S (2013) Processing and properties of macroporous silicon carbide ceramics: a review, Vol 1, Taylor and Francis Ltd., pp 220–242
196. Soy U, Demir A, Caliskan F (2011) Ceram Int 37:15
197. Liang C, Wang Z, Wu L, Zhang X, Wang H, Wang Z (2017) ACS Appl Mater Interfaces 9:29950
198. Jiang Y, Chen Y, Liu YJ, Sui GX (2018) Chem Eng J 337:522
199. Shahzad F, Alhabeb M, Hatter CB, Anasori B, Hong SM, Koo CM, Gogotsi Y (1979) Science 2016(353):1137
200. Iqbal A, Sambyal P, Koo CM (2020) 2D MXenes for electromagnetic shielding: a review, Vol. 30, Wiley-VCH Verlag, p 2000883
201. Song P, Liu B, Qiu H, Shi XT, Cao DP, Gu JW (2021) Compos Commun 24:13
202. Cao MS, Cai YZ, He P, Shu JC, Cao WQ, Yuan J (2019) Chem Eng J 359:1265
203. Han MK, Shuck CE, Rakhmanov R, Parchment D, Anasori B, Koo CM, Friedman G, Gogotsi Y (2020) ACS Nano 14:5008
204. Iqbal A, Shahzad F, Hantanasirisakul K, Kim MK, Kwon J, Hong J, Kim H, Kim D, Gogotsi Y, Koo CM (1979) Science 2020(369):446

205. Wang Q, Xu YM, Bi SY, Lu YX (2021) Chin J Aeronaut 34:103
206. Xu HL, Yin XW, Li XL, Li MH, Liang S, Zhang LT, Cheng LF (2019) ACS Appl Mater Interfaces 11:10198
207. Qi CZ, Wu XY, Liu J, Luo XJ, Zhang HB, Yu ZZ (2023) J Mater Sci Technol 135:213
208. Jin XX, Wang JF, Dai LZ, Liu XY, Li L, Yang YY, Cao YX, Wang WJ, Wu H, Guo SY (2020) Chem Eng J 380:9
209. Wu XY, Han BY, Zhang HB, Xie X, Tu TX, Zhang Y, Dai Y, Yang R, Yu ZZ (2020) Chem Eng J 381:9
210. Yun T, Kim H, Iqbal A, Cho YS, Lee GS, Kim MK, Kim SJ, Kim D, Gogotsi Y, Kim SO, Koo CM (2020) Adv Mater 32:9
211. Zhang JZ, Kong N, Uzun S, Levitt A, Seyedin S, Lynch PA, Qin S, Han MK, Yang WR, Liu JQ, Wang XG, Gogotsi Y, Razal JM (2020) Adv Mater 32:9
212. Liang CB, Qiu H, Song P, Shi XT, Kong J, Gu JW (2020) Sci Bull (Beijing) 65:616
213. Fan Z, Wang D, Yuan Y, Wang Y, Cheng Z, Liu Y, Xie Z (2020) Chem Eng J 381:122696
214. Sambyal P, Iqbal A, Hong J, Kim H, Kim MK, Hong SM, Han MK, Gogotsi Y, Koo CM (2019) ACS Appl Mater Interfaces 11:38046
215. Zhou B, Zhang Z, Li YL, Han GJ, Feng YZ, Wang B, Zhang DB, Ma JM, Liu CT (2020) ACS Appl Mater Interfaces 12:4895
216. Ma ZL, Kang SL, Ma JZ, Shao L, Zhang YL, Liu C, Wei AJ, Xiang XL, Wei LF, Gu JW (2020) ACS Nano 14:8368
217. Zhang X, Wang H, Hu R, Huang C, Zhong W, Pan L, Feng Y, Qiu T, Zhang CJ, Yang J (2019) Appl Surf Sci 484:383
218. Cheng ZL, Chang GJ, Xue B, Xie L, Zheng Q (2023) J Mater Sci Technol 132:132
219. Guo ZZ, Ren PG, Wang J, Hou X, Tang JH, Liu ZB, Chen ZY, Jin YL, Ren F (2023) Chem Eng J 451:12
220. Liang L, Han G, Li Y, Zhao B, Zhou B, Feng Y, Ma J, Wang Y, Zhang R, Liu C (2019) ACS Appl Mater Interfaces 11:25399
221. Liu R, Miao M, Li Y, Zhang J, Cao S, Feng X (2018) ACS Appl Mater Interfaces 10:44787
222. Wang QW, Zhang HB, Liu J, Zhao S, Xie X, Liu LX, Yang R, Koratkar N, Yu ZZ (2019) Adv Funct Mater 29:10
223. Zhang W, Feng Y, Althakafy JT, Liu Y, Abo-Dief HM, Huang M, Zhou L, Su F, Liu C, Shen C (2012) Adv Compos Hybrid Mater 2022:5
224. Gartner TE, Jayaraman A (2019) Modeling and simulations of polymers: a roadmap, Vol 52, American Chemical Society, pp 755–786
225. Van Der Giessen E, Schultz PA, Bertin N, Bulatov VV, Cai W, Csányi G, Foiles SM, Geers MGD, González C, Hütter M, Kim WK, Kochmann DM, Llorca J, Mattsson AE, Rottler J, Shluger A, Sills RB, Steinbach I, Strachan A, Tadmor EB (2020) Roadmap on multiscale materials modeling, Vol 28, Institute of Physics Publishing, p 043001
226. Siochi EJ, Harrison JS (2015) MRS Bull 40:829
227. Yadav R, Tirumali M, Wang X, Naebe M, Kandasubramanian B (2020) Polymer composite for antistatic application in aerospace, Vol 16, China Ordnance Society, pp 107–118
228. Maillard R, Sethio D, Hagemann H, Lawson Daku LM (2019) ACS Omega 4:8786
229. Butler KT, Sai Gautam G, Canepa P (2019) Designing interfaces in energy materials applications with first-principles calculations, Vol 5, Nature Publishing Group, pp 1–12
230. Xiang H, Feng Z, Li Z, Zhou Y (2015) J Appl Phys 117:225902
231. Niethammer C, Becker S, Bernreuther M, Buchholz M, Eckhardt W, Heinecke A, Werth S, Bungartz HJ, Glass CW, Hasse H, Vrabec J, Horsch M (2014) J Chem Theory Comput 10:4455
232. Plimpton S (1995) J Comput Phys 117:1
233. Schwartzentruber TE, Boyd ID (2015) Prog Aerosp Sci 72:66
234. Rao Q, Xiang Y, Leng Y (2013) J Phys Chem C 117:14061
235. Binder K, Egorov SA, Milchev A, Nikoubashman A (2020) Understanding the properties of liquid-crystalline polymers by computational modeling, Vol 3, IOP Publishing Ltd, p 032008
236. Kempfer K, Devémy J, Dequidt A, Couty M, Malfreyt P (2019) ACS Omega 4:5955
237. Liu XL, Crouch IG, Lam YC (2000) Compos Sci Technol 60:857
238. Nurhaniza M, Ariffin MKA, Ali A, Mustapha F, Noraini AW (2010) IOP Conf Ser Mater Sci Eng 11:012010
239. Hu J, Zhang K, Cheng H, Zou P (2020) Chinese J Aeronaut
240. Nilakantan G, Horner S, Halls V, Zheng J (2018) Defence Technol 14:213
241. Cao S, Pang H, Zhao C, Xuan S, Gong X (2020) Compos B Eng 185:107793
242. Slaba TC, Bahadori AA, Reddell BD, Singleterry RC, Clowdsley MS, Blattnig SR (2017) Life Sci Space Res (Amst) 12:1
243. Walsh L, Schneider U, Fogtman A, Kausch C, McKenna-Lawlor S, Narici L, Ngo-Anh J, Reitz G, Sabatier L, Santin G, Sihver L, Straube U, Weber U, Durante M (2019) Life Sci Space Res (Amst) 21:73
244. Narici L, Casolino M, Di Fino L, Larosa M, Picozza P, Rizzo A, Zaconte V (2017) Sci Rep 7:1
245. Kondyurin A (2011) In Journal of Spacecraft and Rockets, American Institute of Aeronautics and Astronautics Inc., pp 378–384
246. Wu L, Song B, Keer LM, Gu L (2018) Crystals (Basel) 8:361
247. Das DK, Sarkar J (2018) Mod Phys Lett B 32:1850075
248. Tserpes K, Kora C (2018) Aerospace 5:106
249. Shin KB, Kim CG, Hong CS, Lee HH (2000) Compos B Eng 31:223
250. Wang C, Cao P, Tang M, Tian W, Liu K, Liu B (2020) Materials 13:2588
251. Bodepati V, Mogulanna K, Rao GS, Vemuri M (2017) In Procedia Engineering, Elsevier Ltd, pp 740–746
252. Capovilla G, Cestino E, Reyneri LM, Romeo G (2020) Aerospace 7:17
253. Astori P, Zanella M, Bernardini M (2020) Aerospace 7:1
254. Dasari SK, Cheddad A, Andersson P (2020) Struct Multidiscip Optim 61:2177
255. Gibney E (2019) Nature 574:22
256. Arute F, Arya K, Babbush R, Bacon D, Bardin JC, Barends R, Biswas R, Boixo S, Brandao FGSL, Buell DA, Burkett B, Chen Y, Chen Z, Chiaro B, Collins R, Courtney W, Dunsworth A, Farhi E, Foxen B, Fowler A, Gidney C, Giustina M, Graff R, Guerin K, Habegger S, Harrigan MP, Hartmann MJ, Ho A, Hoffmann M, Huang T, Humble TS, Isakov SV, Jeffrey E, Jiang Z, Kafri D, Kechedzhi K, Kelly J, Klimov PV, Knysh S, Korotkov A, Kostritsa F, Landhuis D, Lindmark M, Lucero E, Lyakh D, Mandrà S, McClean JR, McEwen M, Megrant A, Mi X, Michielsen K, Mohseni M, Mutus J, Naaman O, Neeley M, Neill C, Niu MY, Ostby E, Petukhov A, Platt JC, Quintana C, Rieffel EG, Roushan P, Rubin NC, Sank D, Satzinger KJ, Smelyanskiy V, Sung KJ, Trevithick MD, Vainsencher A, Villalonga B, White T, Yao ZJ, Yeh P, Zalcman A, Neven H, Martinis JM (2019) Nature 574:505
257. Möller M, Vuik C (2017) Ethics Inf Technol 19:253
258. CSIRO, Growing Australia's quantum technology industry, CSIRO
259. Givi P, Daley AJ, Mavriplis D, Malik M (2020) AIAA J 58:3715
260. Jin X, Al-Qatatsheh A, Subhani K, Salim NV (2021) Chem Eng J 412:128635
261. Ye H, Xian W, Li Y (2021) Machine learning of coarse-grained models for organic molecules and polymers: progress, opportunities, and challenges, Vol 6, American Chemical Society, pp 1758–1772
262. Peerzada M, Abbasi S, Lau KT, Hameed N (2020) Ind Eng Chem Res 59:6375

263. Chung DDL (2019) A review of multifunctional polymer-matrix structural composites, Vol 160, Elsevier Ltd, pp 644–660
264. Pereira T, Guo Z, Nieh S, Arias J, Hahn HT (2009) J Compos Mater 43:549
265. Ladpli P, Nardari R, Kopsaftopoulos F, Chang FK (2019) J Power Sources 414:517
266. Senokos E, Ou Y, Torres JJ, Sket F, González C, Marcilla R, Vilatela JJ (2018) Sci Rep 8:3407
267. Shirshova N, Qian H, Shaffer MSP, Steinke JHG, Greenhalgh ES, Curtis PT, Kucernak A, Bismarck A (2013) Compos Part A Appl Sci Manuf 46:96
268. Fredi G, Jeschke S, Boulaoued A, Wallenstein J, Rashidi M, Liu F, Harnden R, Zenkert D, Hagberg J, Lindbergh G, Johansson P, Stievano L, Asp LE (2018) Multifunctional Materials 1:015003
269. Subhani K, Jin X, Mahon PJ, Kin Tak Lau A, Salim NV (2021) Compos Commun 24:100663
270. Yu Y, Zhang B, Feng M, Qi G, Tian F, Feng Q, Yang J, Wang S (2017) Compos Sci Technol 147:62
271. Yao X, Luan C, Zhang D, Lan L, Fu J (2017) Mater Des 114:424
272. Nasir MA, Akram H, Khan ZM, Shah M, Anas S, Asfar Z, Nauman S (2015) J Intell Mater Syst Struct 26:2362
273. De Simone ME, Andreades C, Meo M, Ciampa F (2019) In Materials Today: Proceedings, Elsevier Ltd, pp 202–209
274. Wan Z, Li JD, Jia M, Li JL (2013) Structural health monitoring (SHM) of three-dimensional braided composite material using carbon nanotube thread sensors, Vol 29, Oxford Academic, pp 617–621
275. Shui X, Chung DDL (2000) J Mater Sci 35:1773
276. Yan DX, Pang H, Li B, Vajtai R, Xu L, Ren PG, Wang JH, Li ZM (2015) Adv Funct Mater 25:559